Stabilizer rank bounds for magic-state orbits

Farrokh Labib[1] and Vincent Russo[1]

[1]*Unitary Foundation*

May 2026

Abstract

Distinct Clifford orbits of magic states can exhibit different stabilizer ranks at small tensor powers. We establish this for qutrits, where the single-qutrit Clifford group has four inequivalent orbits of magic states — Strange, Norrell, Hadamard-eigenstate, and the qutrit T-state — but a nontrivial upper bound on the asymptotic exponent had been pinned down for only the qutrit T-state. For the other three orbits we give explicit stabilizer decompositions, yielding upper bounds on the per-copy asymptotic stabilizer-rank exponent: $\gamma_{\mathrm{S}} \leq \log_3(2)/2 \approx 0.316$ for the Strange state, and $\gamma_{H_3}, \gamma_{\mathbb{N}} \leq \log_3(4)/3 \approx 0.421$ for the Hadamard-eigenstate and Norrell orbits, all strictly below the prior $\gamma_{T_3} \leq 1/2$ baseline. We also prove the first nontrivial $\Omega(m/\log m)$ asymptotic lower bounds for the Hadamard-eigenstate and Norrell orbits, and exhibit two-qutrit Clifford circuits that convert two copies of these states into an injectable phase state with constant success probability, enabling constant-overhead injection of one non-Clifford diagonal gate per orbit. In the case of qubits, we give a closed-form decomposition of the qubit T-type orbit at four copies matching the existing $\gamma_T \leq \log_2(3)/4 \approx 0.396$ exponent via a direct algebraic identity rather than an entangled cat-state construction. An open-source library `stabrank` accompanies the paper, with Lean 4 proof formalizations of all the decompositions.

1 Introduction

Sharp bounds on the classical-simulation cost of Clifford-dominated circuits play a dual role: a fast simulator on a family of circuits rules out a quantum speedup on that family, while a provable lower bound on every simulator certifies one. Stabilizer-rank methods sit at the heart of this story — they reduce the strong-simulation cost of a Clifford circuit with magic-state ancillae to a single quantity, the stabilizer rank of the input magic register, and improvements at any copy count translate directly into faster simulators. The underlying universal model factors an n-qudit circuit into Clifford gates, which are classically simulable in polynomial time [Got98, AG04], and non-Clifford magic-state ancillae [BK05], which supply the resource needed for universal quantum computation.

The relevant invariant is the magic-state stabilizer rank $\chi(|M\rangle^{\otimes t})$, the smallest number of stabilizer states whose linear span contains $|M\rangle^{\otimes t}$. The deterministic algorithm of [BSS16] runs in time $O(p^{\gamma_M t})$ with overhead polynomial in t and in the circuit's qudit count n, where $\gamma_M = \limsup_m \log_p \chi(|M\rangle^{\otimes m})/m$ is the per-copy asymptotic exponent. Every drop in γ_M tightens the

Companion library: `https://github.com/unitaryfoundation/stabrank` [LR26].

best stabilizer-rank simulator; every nontrivial lower bound on γ_M certifies a hard ceiling for the method.

The exponent is invariant under global phase and the Clifford action, so it lives on Clifford orbits of magic states rather than on individual states. For qubits there are two such orbits and both have been studied extensively. For qutrits there are four — Strange, Norrell, Hadamard-eigenstate, and the qutrit T-state — but only the T-state orbit had a nontrivial upper bound on γ_M on record, leaving open whether the four exponents agree, differ, or follow a definite order, and which orbits are operationally usable for magic-state injection.

We resolve this. Explicit small-m stabilizer decompositions, each machine-checked in Lean 4, give $\gamma_{\mathrm{S}} \leq \log_3(2)/2 \approx 0.316$ (the smallest exponent on record across the four qutrit orbits) and $\gamma_{H_3}, \gamma_{\mathbb{N}} \leq \log_3(4)/3 \approx 0.421$, all strictly below the prior $\gamma_{T_3} \leq 1/2$ baseline. Transferring the subset-sum argument of [LS22] to qutrits gives the first nontrivial $\Omega(m/\log m)$ lower bounds for the Hadamard-eigenstate and Norrell orbits. Two-copy probabilistic conversion circuits route the Hadamard-eigenstate and Norrell upper bounds into magic-state injection, supplying constant-overhead access to one non-Clifford diagonal gate per orbit. For Strange the corresponding search returns only Clifford outputs — a rigidity that we prove cannot be bypassed by any two-qutrit Clifford and ancilla measurement, so the smallest qutrit exponent on record is currently not operationally accessible. A short qubit appendix gives a closed-form four-copy T-type decomposition matching the $\gamma_T \leq \log_2(3)/4 \approx 0.396$ exponent of [QPG21] via direct algebra rather than entangled cat-state chains.

Stabilizer states. For an odd prime p, an n-qudit stabilizer state has the canonical form

$$|\sigma\rangle = \frac{1}{\sqrt{p^k}} \sum_{y \in \mathbb{F}_p^k} \omega_p^{Q(y)} |x_0 + Wy\rangle, \tag{1}$$

with $\omega_p = e^{2\pi i/p}$ a primitive p-th root of unity, $x_0 \in \mathbb{F}_p^n$, $W \in \mathbb{F}_p^{n\times k}$ of full column rank, and $Q : \mathbb{F}_p^k \to \mathbb{F}_p$ a polynomial of degree at most 2 (i.e. admitting linear and constant terms) [Got99, HDDM05]; we write $\mathrm{Stab}_n^{(p)}$ for the set of n-qudit stabilizer states. The n-qudit Clifford group $\mathrm{Cl}(n,p)$ is the normalizer of the Pauli group in the unitary group on $(\mathbb{C}^p)^{\otimes n}$ and acts transitively on $\mathrm{Stab}_n^{(p)}$. For any pure state $|\psi\rangle$, its *projective Clifford orbit* is

$$\mathcal{O}_{|\psi\rangle} = \{e^{i\theta} U|\psi\rangle : U \in \mathrm{Cl}(n,p),\ \theta \in \mathbb{R}\}. \tag{2}$$

A pure state is a *magic state* if it is not a stabilizer state, and the orbit of any magic state consists entirely of non-stabilizer states.

The classical cost of simulating such a circuit on t copies of a magic state $|M\rangle$ is controlled by the *stabilizer rank*

$$\chi(|\psi\rangle) = \min\left\{r : |\psi\rangle = \sum_{i=1}^{r} c_i |\sigma_i\rangle,\ |\sigma_i\rangle \in \mathrm{Stab}_n^{(p)},\ c_i \in \mathbb{C}\right\}, \tag{3}$$

the smallest number of stabilizer states whose linear span contains $|\psi\rangle$ [BSS16, BG16, BBC$^+$19]: the deterministic stabilizer-rank algorithm of [BSS16] runs in time $O(p^{\gamma_M t})$ with overhead polynomial in t and in the number n of qudits in the circuit, where the per-copy asymptotic exponent

$$\gamma_M = \limsup_{m\to\infty} \frac{\log_p \chi(|M\rangle^{\otimes m})}{m} \tag{4}$$

governs the dominant cost. The stabilizer rank is invariant under global phase and the Clifford action, so γ_M via (4) is well-defined on Clifford orbits of magic states.

Qubits. For qubits ($p = 2$) the single-qubit Clifford group has two inequivalent orbits of magic states, the H-type and T-type orbits of [BK05]. The best exact-rank upper-bound exponent for the H-type is $\gamma_H \leq \log_2(3)/4 \approx 0.396$ via the contracted-cat-state construction of [QPG21,Qas20][1]; the strongest exact-rank lower bounds give only $\Omega(m)$ growth [PSV22,Lab22,LS22]. On the approximate-rank side, the qubit landscape is sharper: a $\tilde{\Omega}(m^2)$ probabilistic lower bound [MT23] and a Barnes–Wall-lattice lower bound [KS25] have both appeared recently. The contracted-cat-state construction of [QPG21] is generalized in the same paper to the T-type orbit, establishing $\gamma_T \leq \log_2(3)/4$ asymptotically; however, that argument proceeds by contracting chains of entangled cat states and does not give an explicit small-m decomposition.

We establish the orbit-dependence of stabilizer rank in qubits (Section 2.1). The H-type value $\chi(|H\rangle^{\otimes 4}) = 4$ by an exhaustive triple-search distributed with the library (giving equality using the upper bound of [BSS16]); for the T-type orbit we give an explicit algebraic decomposition showing $\chi(|T\rangle^{\otimes 4}) \leq 3$ (Appendix C.4), matching the asymptotic exponent $\gamma_T \leq \log_2(3)/4 \approx 0.396$ of [QPG21] via an explicit small-m identity rather than an entangled-cat-state chain. The two qubit orbits therefore have provably distinct stabilizer ranks at $m = 4$.

Qutrits. For qutrits ($p = 3$) the single-qutrit Clifford group has four inequivalent orbits of magic states [VMGE14, JP20]: the Strange, Norrell[2], Hadamard-eigenstate, and qutrit T-state orbits, with representatives

$$
\begin{aligned}
|\mathbb{S}\rangle &= \frac{1}{\sqrt{2}}(|1\rangle - |2\rangle), & |H_3\rangle &= \frac{1}{\sqrt{3-\sqrt{3}}}\Big(|0\rangle + \frac{\sqrt{3}-1}{2}(|1\rangle + |2\rangle)\Big), \\
|\mathbb{N}\rangle &= \frac{1}{\sqrt{6}}(|0\rangle + |1\rangle - 2|2\rangle), & |T_3\rangle &= \frac{1}{\sqrt{3}}(|0\rangle + \omega_9|1\rangle + \omega_9^2|2\rangle),
\end{aligned}
\tag{5}
$$

with $\omega_9 = e^{2\pi i/9}$. Each orbit has a distinct role in the qutrit literature. The qutrit T-state $|T_3\rangle$ is the standard phase-hierarchy magic state, injected via the diagonal qutrit T-rotation $\mathrm{diag}(1, \omega_9, \omega_9^2)$ [HV12] used in fault-tolerant qutrit architectures [ACB12,CAB12,DH15]; the Hadamard-eigenstate $|H_3\rangle$ is the $+1$ eigenvector of the qutrit Hadamard; the Strange state $|\mathbb{S}\rangle$ is a $d = 3$ SIC-POVM fiducial [App05, Zhu10]; and the Norrell state $|\mathbb{N}\rangle$ was introduced alongside $|\mathbb{S}\rangle$ in [VMGE14].

The four orbits give four exponents $\gamma_{\mathbb{S}}, \gamma_{H_3}, \gamma_{\mathbb{N}}, \gamma_{T_3}$, and prior to this work almost none of them were pinned down: the only nontrivial exact-stabilizer-rank upper-bound exponent on record was $\gamma_{T_3} \leq 1/2$, which follows from the numerically established two-copy bound $\chi(|T_3\rangle^{\otimes 2}) \leq 3$ of [KS21] by sub-multiplicativity. The same paper additionally reports $\chi(|T_3\rangle^{\otimes 3}) \leq 8$ (marked there as numerical rather than rigorous). The other three qutrit orbits had no nontrivial stabilizer-rank bounds in either direction prior to this work; whether the four qutrit exponents differ, or are all equal, was open at every orbit.

For the three non-T_3 qutrit orbits we give explicit stabilizer decompositions establishing $\gamma_{\mathbb{S}} \leq \log_3(2)/2 \approx 0.316$ (the smallest known exact-rank upper-bound exponent across the four orbits) and $\gamma_{H_3}, \gamma_{\mathbb{N}} \leq \log_3(4)/3 \approx 0.421$, all strictly below the $\gamma_{T_3} \leq 1/2$ baseline. On the lower-bound side we transfer the subset-sum argument of [LS22] to qutrits and obtain the first nontrivial

[1] The naming convention of [BK05] used here calls the edge-of-octahedron orbit H-type and the face-of-octahedron orbit T-type. The convention of [QPG21,Qas20] swaps these names: their $|T\rangle$ is the edge-of-octahedron phase state (our H-type) and their $|F\rangle$ is the face-center state (our T-type). All asymptotic exponents we attribute to [QPG21] use the translation accordingly.

[2] The Strange and Norrell representatives were introduced in [VMGE14] (which built on the resource framework of [VFGE12, HWVE14]); the four-orbit Clifford classification was systematized in [JP20]. The "Strange" and "Norrell" names appear to be drawn from Susanna Clarke's 2004 novel *Jonathan Strange & Mr Norrell*, whose two protagonists are English magicians.

$\Omega(m/\log m)$ asymptotic lower bounds on $\chi(|H_3\rangle^{\otimes m})$ and $\chi(|\mathbb{N}\rangle^{\otimes m})$. Exhaustive computer search additionally certifies several small-m tight values, including $\chi(|\mathbb{S}\rangle^{\otimes 3}) = 4$ (Theorem 3).

Magic state injection. The four qutrit orbits also differ in how the rank improvements translate to circuit-runtime improvements. None of $|\mathbb{S}\rangle$, $|H_3\rangle$, $|\mathbb{N}\rangle$ is a phase state (a state of the form $\frac{1}{\sqrt{p}}\sum_j e^{i\theta_j}|j\rangle$ with uniform-modulus amplitudes), so standard single-shot two-qutrit Clifford injection via a diagonal gate [ACB12, HV12, CGK17] does not apply. We exhibit explicit two-copy probabilistic conversion protocols (Theorem 6): for $|H_3\rangle$ and $|\mathbb{N}\rangle$, a fixed two-qutrit Clifford applied to $|M\rangle \otimes |M\rangle$ followed by a computational-basis measurement on the second qutrit projects to a phase state on the first qutrit with constant success probability (3/8 and 1/4 respectively), after which standard single-shot injection produces a non-Clifford diagonal gate. This supplies a constant-overhead route to phase-state injection for those two orbits. For $|\mathbb{S}\rangle$ the corresponding search returns only Clifford outputs, so the smaller $|\mathbb{S}\rangle$ upper-bound exponent is not currently usable as a runtime improvement under this consumption model. Both failures trace to the same support-2 equal-modulus orbit structure documented in Proposition 5.

The open-source `stabrank` software package (Section 4) accompanies the paper, providing the simulated-annealing search that produced the decompositions, the exhaustive lower-bound certificate pipeline, and Lean 4 [dMU21] + mathlib4 [The20] formalizations of every qutrit decomposition identity in Appendix C.

2 Stabilizer-rank bounds

We prove that the stabilizer rank of tensor powers of a magic state is orbit-dependent, first in qubits (Section 2.1) and then in qutrits (Section 2.2). Stabilizer rank is sub-multiplicative under tensor product, $\chi(\psi \otimes \phi) \leq \chi(\psi)\chi(\phi)$, since concatenating decompositions of ψ and ϕ produces a length-product decomposition of $\psi \otimes \phi$. Iterating, any finite-m bound $\chi(|M\rangle^{\otimes m}) \leq r$ gives $\chi(|M\rangle^{\otimes mk}) \leq r^k$ for every $k \geq 1$, and so

$$\gamma_M \leq \log_p(r)/m. \tag{6}$$

2.1 Qubit orbit-dependent bounds

The two Clifford-inequivalent qubit magic-state orbits of [BK05] already exhibit distinct stabilizer ranks at small m. The H-type orbit corresponds to the edges of the stabilizer octahedron on the Bloch sphere, with phase-state representative $(|0\rangle + e^{i\pi/4}|1\rangle)/\sqrt{2}$ used throughout the qubit T-gate distillation literature (Clifford-equivalent to $|H\rangle = \cos(\pi/8)|0\rangle + \sin(\pi/8)|1\rangle$). The T-type orbit corresponds to the faces of the stabilizer octahedron, with Bloch vector $(1,1,1)/\sqrt{3}$ and representative $|T\rangle = \cos\beta|0\rangle + e^{i\pi/4}\sin\beta|1\rangle$ where $\cos(2\beta) = 1/\sqrt{3}$.

Proposition 1.

$$\chi\Big(|H\rangle^{\otimes 4}\Big) = 4 \qquad \textit{and} \qquad \chi\Big(|T\rangle^{\otimes 4}\Big) = 3. \tag{7}$$

The H-type decomposition giving $\chi(|H\rangle^{\otimes 4}) \leq 4$ is tabulated in [BSS16]; the matching lower bound $\chi(|H\rangle^{\otimes 4}) \geq 4$, and hence the equality $\chi(|H\rangle^{\otimes 4}) = 4$, is certified by the exhaustive triple-search distributed with the library. The T-type value $\chi(|T\rangle^{\otimes 4}) = 3$ is Proposition 8, proved by an explicit algebraic decomposition in Appendix C.4 and established as tight via the $m = 3$ lower-bound certificate by monotonicity.

The T-type value $\chi(|T\rangle^{\otimes 4}) = 3$ at $m = 4$ is strictly below the H-type tight value $\chi(|H\rangle^{\otimes 4}) = 4$ at the same m, but this is a local algebraic phenomenon and not (yet) an asymptotic separation. The decomposition that achieves the T-type bound is a specific identity in twelfth roots of unity that has no obvious H-type analogue. The values for $m \geq 5$ for the T-type orbit reported in Table 1 are sub-multiplicativity extensions of $\chi(|T\rangle^{\otimes 4}) = 3$, not independent bounds; whether genuinely smaller rank witnesses exist at $m \in \{5, 6\}$ is unknown, as is whether the asymptotic exponents γ_H and γ_T in fact coincide.

Table 1 summarizes the state of knowledge for both orbits at small m, combining our new bounds with the H-type values of [QPG21].

m	1	2	3	4	5	6
$\chi(\lvert H\rangle^{\otimes m})$	2	$2^\dagger$	$3^\dagger$	$4^\dagger$	$\leq 6^\dagger$	$\leq 6^*$
$\chi(\lvert T\rangle^{\otimes m})$	2	$2^\ddagger$	$3^\ddagger$	$3^\ddagger$	$\leq 6^\ddagger$	$\leq 6^\ddagger$

Table 1: Stabilizer rank bounds for the two qubit magic-state orbits at small m. Entries marked ‡ are new contributions of this work; other entries are from [BSS16] (†) and [QPG21] (*). The unmarked $\chi = 2$ entries at $m = 1$ follow from the fact that any non-stabilizer single-qubit state has stabilizer rank exactly 2.

2.2 Qutrit upper bounds

Our first bound is specific to $|\mathbb{S}\rangle$ at $m = 2$. The two-copy state $|\mathbb{S}\rangle^{\otimes 2}$ is supported on the four computational-basis vectors in $\{1, 2\}^2$, where it equals $\frac{1}{2}(|11\rangle - |12\rangle - |21\rangle + |22\rangle)$; this four-term superposition admits an explicit two-term stabilizer-state decomposition, dropping the rank below the trivial product bound $\chi(|\mathbb{S}\rangle)^2 = 4$.

Theorem 2. *For* $|\mathbb{S}\rangle$,

$$\chi(|\mathbb{S}\rangle^{\otimes 2}) = 2 \quad \textit{and} \quad \gamma_{\mathbb{S}} \leq \log_3(2)/2 \approx 0.316. \tag{8}$$

The witness for the rank bound is

$$|\mathbb{S}\rangle^{\otimes 2} = -\frac{i\sqrt{3}}{2}\omega_3\big(|\sigma_1\rangle - |\sigma_2\rangle\big), \tag{9}$$

where $|\sigma_1\rangle, |\sigma_2\rangle$ *are the two-qutrit stabilizer states of the canonical form* (1) *with* $k = 2$, $x_0 = 0$, $W = I_2$, *and quadratic forms* $Q_1(y) = y_0^2 + y_0y_1 + y_1^2$, $Q_2(y) = y_0^2 + 2y_0y_1 + y_1^2$. *The exponent bound follows by* (6).

The proof is in Appendix C.1.1. The exponent bound in (8) is the smallest known exact-rank upper-bound exponent across the four orbits, strictly below the $\gamma_{T_3} \leq 1/2$ baseline of [KS21]. The closest comparable result in the literature, $\chi'(|T_3\rangle^{\otimes t}) \leq 3^{0.32t}$ of [HL19], is on the approximate rank, not exact, and applies to a different orbit. The decomposition in (9) exploits $|\mathbb{S}\rangle$'s rank-one single-qutrit support on $\{1, 2\}$; the orbits $|H_3\rangle$ and $|\mathbb{N}\rangle$ have full single-qutrit support on $\{0, 1, 2\}$, and the analogous $m = 2$ collapse does not occur. Each of the three non-T_3 orbits, however, admits an explicit four-term decomposition at $m = 3$.

Theorem 3. *For each* $|M\rangle \in \{|\mathbb{S}\rangle, |H_3\rangle, |\mathbb{N}\rangle\}$,

$$\chi(|M\rangle^{\otimes 3}) = 4 \quad \textit{and} \quad \gamma_M \leq \log_3(4)/3 \approx 0.4206. \tag{10}$$

The equality in (10) combines an upper bound with an exhaustive lower-bound certificate. The upper bound $\chi(|M\rangle^{\otimes 3}) \leq 4$ is established by orbit-specific four-term stabilizer decompositions, one per orbit, proved in Appendix C.1.2 ($|\mathbb{S}\rangle$), Appendix C.2.2 ($|H_3\rangle$), and Appendix C.3.2 ($|\mathbb{N}\rangle$). For $|H_3\rangle$ and $|\mathbb{N}\rangle$ this is the first nontrivial exact-rank asymptotic upper bound. The $|\mathbb{S}\rangle$ $m = 3$ decomposition does not improve on the $|\mathrm{S}\rangle$ exponent of Theorem 2 ($\log_3(4)/3 > \log_3(2)/2$); it is needed to certify the $\chi(|\mathbb{S}\rangle^{\otimes 3}) = 4$ equality below. The lower bound $\chi(|M\rangle^{\otimes 3}) \geq 4$ comes from an exhaustive enumeration of unordered triples from the canonical-form three-qutrit stabilizer-state dictionary $\mathcal{D}_3$. The dictionary lists $|\mathcal{D}_3| = 41{,}580$ canonical-form tuples (k, x_0, W, Q), a slight overcount of the $3^3 \prod_{j=1}^{3}(3^j + 1) = 30{,}240$ distinct projective three-qutrit stabilizer states; the redundancy comes from phase-polynomial overparametrization (different canonical-form tuples can yield the same state vector) and only strengthens the non-existence certificate. Exhausting the $\binom{41{,}580}{3} \approx 1.2 \times 10^{13}$ unordered triples rules out $\chi(|M\rangle^{\otimes 3}) \leq 3$. The certificate machinery and accompanying companion bounds at other m are part of the `stabrank` library (Section 4).

Together with the prior $|T_3\rangle$ bounds of [KS21] and exhaustive small-m search certificates for the $|T_3\rangle$, $|H_3\rangle$, and $|\mathbb{N}\rangle$ entries at $m \leq 3$, Table 2 consolidates the current status of $\chi(|M\rangle^{\otimes m})$ across the four orbits.

m	1	2	3	4
$\chi(\lvert\mathbb{S}\rangle^{\otimes m})$	2	$2^{\ddagger}$	$4^{\ddagger}$	≤ 4
$\chi(\lvert H_3\rangle^{\otimes m})$	2	$3^{\ddagger}$	$4^{\ddagger}$	≤ 8
$\chi(\lvert\mathbb{N}\rangle^{\otimes m})$	2	$3^{\ddagger}$	$4^{\ddagger}$	$\leq 7^{\ddagger}$
$\chi(\lvert T_3\rangle^{\otimes m})$	$3^{\ddagger}$	3^{*}	$\leq 8^{*}$	≤ 9

Table 2: Stabilizer-rank values and upper bounds across the four qutrit magic-state orbits at small m. Entries marked ‡ are contributions of this work; those marked * are due to [KS21]. Trivial bounds that follow from sub-multiplicativity are left unmarked. The $\chi(|T_3\rangle) = 3$ entry at $m = 1$ combines the trivial computational-basis upper bound $\chi(|T_3\rangle) \leq 3$ with an exhaustive pair-search certificate ruling out $\chi(|T_3\rangle) \leq 2$.

2.3 Asymptotic lower bounds

The non-uniform amplitudes of $|H_3\rangle$ and $|\mathbb{N}\rangle$ that foreclose the $m = 2$ support-collapse trick used for $|\mathrm{S}\rangle$ also enable an asymptotic lower bound via a subset-sum argument, adapted from the qubit-T-state technique of [LS22]. The technique requires two of the nonzero amplitudes of $|\psi\rangle$ to have moduli that differ by a factor of at least 2, so that the $m+1$ distinct moduli appearing in $|\psi\rangle^{\otimes m}$ form an exponentially increasing sequence. This hypothesis holds for $|H_3\rangle$ ($|a_0|/|a_1| = \sqrt{3}+1 \approx 2.73$) and $|\mathbb{N}\rangle$ ($|a_2|/|a_0| = 2$), but fails for $|\mathbb{S}\rangle$, whose two nonzero amplitudes share the modulus $1/\sqrt{2}$.

Proposition 4. *Let $|\psi\rangle = a_0|0\rangle + a_1|1\rangle + a_2|2\rangle \in \mathbb{C}^3$ be a single-qutrit state for which there exist indices $i, j \in \{0,1,2\}$ with $a_i \neq 0$, $a_j \neq 0$, and $|a_i|/|a_j| \geq 2$. Then*

$$\chi(|\psi\rangle^{\otimes m}) \geq \frac{m+1}{3\log_2(m+1)} \in \Omega\left(\frac{m}{\log m}\right). \tag{11}$$

In particular, $\chi(|H_3\rangle^{\otimes m}), \chi(|\mathbb{N}\rangle^{\otimes m}) \in \Omega(m/\log m)$.

Proof. A qutrit stabilizer state $|\sigma\rangle$ on m qutrits has the canonical form

$$|\sigma\rangle = 3^{-k/2} \sum_{y \in \mathbb{F}_3^k} \omega^{Q(y)} |x_0 + Wy\rangle, \tag{12}$$

for some $k \in \{0, \ldots, m\}$, affine offset x_0, isometric embedding $W \in \mathbb{F}_3^{m \times k}$, and quadratic form $Q : \mathbb{F}_3^k \to \mathbb{F}_3$, with $\omega = e^{2\pi i/3}$. Each coordinate of $|\sigma\rangle$ therefore lies in $\{0, 3^{-k/2}\omega^j : j \in \{0,1,2\}\}$. Given a decomposition $|\psi\rangle^{\otimes m} = \sum_{i=1}^r c_i |\sigma_i\rangle$ of length $r = \chi(|\psi\rangle^{\otimes m})$, write $\tilde{c}_i = 3^{-k_i/2} c_i$; then for every coordinate $x \in \mathbb{F}_3^m$,

$$\langle x|\psi^{\otimes m}\rangle = \sum_{i=1}^{r} \varepsilon_{i,x} \tilde{c}_i. \tag{13}$$

The coefficients $\varepsilon_{i,x}$ take values in $\{0, 1, \omega, \omega^2\}$, so each coordinate of $|\psi\rangle^{\otimes m}$ is a subset-sum of the $3r$-tuple $(\tilde{c}_i, \omega\tilde{c}_i, \omega^2\tilde{c}_i)_{i=1}^r$, yielding a subset-sum representation of length $3r$ of the coordinate vector. The factor of 3 counts the three cube-roots of unity $\{1, \omega, \omega^2\}$ appearing as $\varepsilon_{i,x}$ values; the qubit version of this argument lifts each $\tilde{c}_i$ to four entries $\{\pm\tilde{c}_i, \pm i\tilde{c}_i\}$ and yields a $4r$-tuple instead. By the subset-sum lower bound of [LS22, Theorem 3.1], any subset-sum representation of a q-tuple containing an exponentially increasing subsequence of length ℓ (i.e., ℓ entries whose absolute values each at least double the previous) has length at least $\ell / \log_2 \ell$. Hence $3r \geq \ell / \log_2 \ell$, giving $\chi(|\psi\rangle^{\otimes m}) \geq \ell / (3 \log_2 \ell)$.

It remains to produce an exponentially increasing subsequence of length $\ell = m + 1$ in the coordinates of $|\psi\rangle^{\otimes m}$. By hypothesis, there exist indices $i_a, i_b \in \{0,1,2\}$ with $a = |a_{i_a}|$, $b = |a_{i_b}|$, $a \geq 2b > 0$. For each $k \in \{0, \ldots, m\}$, set

$$x^{(k)} = (\underbrace{i_a, \ldots, i_a}_{k}, \underbrace{i_b, \ldots, i_b}_{m-k}) \in \mathbb{F}_3^m, \qquad \text{so that} \qquad \left|\langle x^{(k)}|\psi^{\otimes m}\rangle\right| = a^k b^{m-k}. \tag{14}$$

The $m + 1$ values $\{a^k b^{m-k}\}_{k=0}^m$ are distinct and form an exponentially increasing sequence of consecutive ratio $a/b \geq 2$, so we may take $\ell = m + 1$ in (11). □

The proof above is a direct adaptation of the qubit-T-state argument of [LS22, Theorem 3.1]: the only technical change is the factor of 3 in place of 4 in the subset-sum coefficient count, accounting for cube-roots of unity in the qutrit canonical form rather than fourth-roots. What is new here is the state-specific verification: which qutrit orbits satisfy the modulus-ratio hypothesis ($|H_3\rangle$ and $|\mathbb{N}\rangle$ do, as recorded above), and which provably do not. The $|\mathbb{S}\rangle$-orbit exclusion is the latter; we record it as a separate rigidity proposition below.

Proposition 5. *Let $\mathcal{O}_S \subset \mathbb{C}^3$ denote the projective Clifford orbit of $|\mathbb{S}\rangle$ under $\mathrm{Cl}(1,3)$. Then: (i) every $|\phi\rangle \in \mathcal{O}_S$ has support of cardinality 2 with the two nonzero amplitudes of equal modulus; and (ii) $|\mathcal{O}_S| = 9$, with the orbit consisting of the three nontrivial 2-element supports of $\mathbb{F}_3$ and three discrete phase choices per support. Consequently, the modulus-ratio hypothesis of Proposition 4 fails at every Clifford representative of $|\mathbb{S}\rangle$, and Proposition 4 yields no asymptotic lower bound on $\chi(|\mathbb{S}\rangle^{\otimes m})$.*

The full proof is in Appendix B. The same property that prevents the subset-sum argument for $|\mathbb{S}\rangle$ is what makes $|\mathbb{S}\rangle$ admit the smallest known exact-rank upper-bound exponent across the four orbits ($\gamma_{\mathbb{S}} \leq \log_3(2)/2$, by Theorem 2); closing the gap for $|\mathbb{S}\rangle$ requires a different lower-bound technique. The asymptotic growth $\Omega(m/\log m)$ established for $|H_3\rangle$ and $|\mathbb{N}\rangle$ above is weaker than the $\Omega(m)$ lower bound of [Lab22] for a specific qudit-T-gate magic state, but applies to representatives of orbits that prior work does not cover. The algebraic-symmetry arguments underlying Proposition 5 are reminiscent of the stabilizer-polytope symmetry analysis of [HG19], which exploits the same Clifford-orbit structure to compute robustness-of-magic on small qudit systems.

3 Magic-state injection

The stabilizer-rank exponents of Section 2 bound the state-vector cost of the deterministic stabilizer-rank simulator of [BSS16] applied directly to $|M\rangle^{\otimes m}$. Converting them to a circuit-runtime advantage on a concrete Clifford-plus-$|M\rangle$ circuit additionally requires a model for consuming the magic-state ancilla. The standard choice is a *deterministic injection gadget*: a fixed entangling two-qutrit Clifford that, on a chosen ancilla measurement outcome, applies a non-Clifford gate to the data and corrects the remaining outcomes via Clifford byproducts. For T_3 the diagonal qutrit T-rotation $\mathrm{diag}(1, \omega_9, \omega_9^2)$ supplies one, so $\gamma_{T_3} \leq 1/2$ is a circuit-runtime bound.

For the three non-T_3 orbits, standard single-shot injection via a diagonal gate requires the magic state to be a *phase state* (i.e. have uniform amplitudes up to phases) [ACB12, HV12, CGK17]. Since $|\mathbb{S}\rangle$, $|H_3\rangle$, and $|\mathbb{N}\rangle$ all have non-uniform amplitudes, this route is closed [Pra20, PG20].

3.1 Two-copy probabilistic conversion

A milder construction [BK05, ACB12], introduced for the qubit phase state $(|0\rangle + e^{i\pi/4}|1\rangle)/\sqrt{2}$ (the standard "T-state" of the qubit distillation literature, in our convention an H-type representative) and adapted to the qutrit Hadamard-eigenstate, instead feeds two copies of $|M\rangle$ into a two-qutrit Clifford, measures the second qutrit, and recovers a Clifford-equivalent phase state on the first qutrit on a designated branch. The recovered phase state is then injected via the standard single-shot gadget. The resulting pipeline consumes $2/q$ copies of $|M\rangle$ in expectation per non-Clifford gate, where q is the branch success probability: an $O(1)$ ancilla overhead provided (a) such a Clifford exists and (b) the recovered phase state implements a non-Clifford gate under standard injection. The phase state that emerges in Theorem 6 below implements one specific non-Clifford diagonal gate per orbit (the $|H_3\rangle$ and $|\mathbb{N}\rangle$ gates listed in (16) and (19)); reaching other non-Clifford diagonal targets requires an additional gate-synthesis step on top of the two-copy primitive.

A complete enumeration over $\mathrm{Sp}(4, \mathbb{F}_3) \times \mathbb{F}_3$ (the choice of Clifford and choice of measurement outcome, modulo the Heisenberg–Weyl prefactor as in Appendix A) settles the existence question for every non-T_3 orbit:

Theorem 6. *For $|M\rangle \in \{|H_3\rangle, |\mathbb{N}\rangle\}$ there exist two-qutrit Cliffords C and measurement branches k such that $\langle k|_{\mathrm{anc}} C(|M\rangle \otimes |M\rangle)$ is proportional to a phase state whose standard single-shot injection yields a non-Clifford diagonal gate. For $|M\rangle = |\mathbb{S}\rangle$ no such protocol exists: every C that maps $|\mathbb{S}\rangle \otimes |\mathbb{S}\rangle$ to a phase state injects a Clifford gate.*

Proof. By exhaustive search over the symplectic-quotient representation (Lemma 7), one identifies valid protocols for $|H_3\rangle$ and $|\mathbb{N}\rangle$. The raw search outputs the following two-qutrit Cliffords:

$$\begin{aligned} C_{|H_3\rangle} &= H_1 \mathrm{SUM} H_1 \mathrm{SUM} H_1 S_2 \mathrm{SUM} H_1 H_2^2, \\ C_{|\mathbb{N}\rangle} &= H_1 H_2 \mathrm{SUM} H_1^\dagger H_2 \mathrm{SUM} H_1. \end{aligned} \tag{15}$$

Hadamard-eigenstate protocol. Let $N = \sqrt{3 - \sqrt{3}}$ and $c = (\sqrt{3} - 1)/2$ (the same constants used throughout Appendix C.2). The two-copy input state is $|H_3\rangle \otimes |H_3\rangle$, where the single-copy Hadamard-eigenstate is $|H_3\rangle = \frac{1}{N}\big(|0\rangle + c|1\rangle + c|2\rangle\big)$. Applying the two-qutrit Clifford $C_{|H_3\rangle}$ to this input state and projecting the ancilla (leg 2) onto the outcome $k = 1$ yields the data-qutrit output vector

$$|\psi_{k=1}\rangle = \langle 1|_{\mathrm{anc}} C_{|H_3\rangle}(|H_3\rangle \otimes |H_3\rangle) = \frac{\lambda}{\sqrt{3}}\big(|0\rangle + e^{i\pi/2}|1\rangle + e^{i\pi/3}|2\rangle\big), \tag{16}$$

where $\lambda \in \mathbb{C}$ is a normalization scalar satisfying $|\lambda|^2 = 3/8$. Since all three amplitudes of the post-selected state have equal modulus, it is a phase state. The relative phases are $\arg(\psi_1/\psi_0) = \pi/2$ and $\arg(\psi_2/\psi_0) = \pi/3$, corresponding to the single-qutrit diagonal gate $\mathrm{diag}(1, i, e^{i\pi/3})$. Since a single-qutrit diagonal Clifford gate must have phases that are multiples of $2\pi/3$, the phase $\pi/2$ certifies that the injected gate is non-Clifford.

Norrell protocol. The two-copy input state is $|\mathbb{N}\rangle \otimes |\mathbb{N}\rangle$, where $|\mathbb{N}\rangle = \frac{1}{\sqrt{6}}(|0\rangle + |1\rangle - 2|2\rangle)$ in the computational basis. First, the gate H_1 acts on the data qutrit as the qutrit Fourier transform, leaving the ancilla unchanged. On the amplitudes $v_{a,b} = c_N(a)c_N(b)/6$ (where $c_N = (1, 1, -2)^T$), the data Fourier transform produces

$$|\Psi_1\rangle = (H_1 \otimes \mathbb{1})(|\mathbb{N}\rangle \otimes |\mathbb{N}\rangle) = \frac{1}{6\sqrt{3}} \sum_{j,b} \hat{c}(j) c_N(b) |j, b\rangle, \tag{17}$$

where the inner sum evaluates using $1 + \omega + \omega^2 = 0$ as

$$\hat{c}(j) = \sum_{a=0}^{2} \omega^{aj} c_N(a) = 1 + \omega^j - 2\omega^{2j}. \tag{18}$$

This evaluates to $\hat{c}(0) = 0$, $\hat{c}(1) = -3\omega^2$, and $\hat{c}(2) = -3\omega$. Thus, after H_1, only the data components with $j \in \{1, 2\}$ survive.

Applying the remaining gates of $C_{|\mathbb{N}\rangle}$ and projecting onto the ancilla outcome $k = 0$ yields

$$|\psi_{k=0}\rangle = \langle 0|_{\mathrm{anc}} C_{|\mathbb{N}\rangle} (|\mathbb{N}\rangle \otimes |\mathbb{N}\rangle) = \frac{\mu}{\sqrt{3}} \big(|0\rangle - |1\rangle - |2\rangle\big), \tag{19}$$

with $|\mu|^2 = 1/4$, confirming a success probability of $1/4$ to obtain a phase state. The relative phases are both π, defining the injected diagonal gate $\mathrm{diag}(1, -1, -1)$. Because π is not a multiple of $2\pi/3$, this gate is non-Clifford.

Finally, for $|M\rangle = |\mathrm{S}\rangle$, an exhaustive search confirms that no two-copy conversion protocol exists: every (C, k) pair that maps $|\mathrm{S}\rangle \otimes |\mathrm{S}\rangle$ to a phase state yields relative phases restricted to the Clifford-trivial ones. □

Unlike the qubit case [BK05, Sec. III], where the Hadamard gate naturally pair-conjugates real amplitudes to equalize their moduli, the qutrit Fourier transform has no such conjugate-pairing property. Modulus equalization for $|H_3\rangle$ and $|\mathbb{N}\rangle$ therefore requires the longer alternating sequences of Hadamards, SUMs, and phase gates in (15).

Operationally, Theorem 6 provides a constant-overhead route from copies of $|M\rangle \in \{|H_3\rangle, |\mathbb{N}\rangle\}$ to one specific non-Clifford diagonal gate per orbit ($\mathrm{diag}(1, i, e^{i\pi/3})$ and $\mathrm{diag}(1, -1, -1)$ respectively). Arbitrary diagonal targets outside this image require additional gate-synthesis overhead.

For $|\mathrm{S}\rangle$, the best upper-bound exponent ($\gamma_{\mathrm{S}} \leq \log_3(2)/2$) remains operationally inaccessible under deterministic single-shot injection, two-copy probabilistic conversion and even three-copy protocols: an exhaustive search over the 3-qutrit symplectic group using coset pruning identifies no protocols to obtain a non-Clifford diagonal gate.

4 The `stabrank` library

The numerical and verification work in this paper is carried out in `stabrank`, an open-source Python package with a C++ core released with the manuscript. The library has a heuristic upper-bound stage (simulated-annealing decomposition search, hereafter SA) and two exhaustive stages

(the k-tuple enumeration that produces rank lower-bound certificates and the symplectic-quotient sweep behind the gadget non-existence result of Section 3). The SA search is treated as untrusted scaffolding: its output is a candidate canonical-form decomposition that is then replayed against an independent verifier; the search itself never enters the verification path. Table 3 maps each paper result to its producing artifact and audit channels, and Figure 1 sketches the upper-bound pipeline.

Result	Producing artifact	Auditing channel(s)
Thm. 2	SA decomposition	numerical; Lean 4
Prop. 4	analytic proof	—
Thm. 3 (≤ 4)	SA decomposition	numerical; Lean 4
Thm. 3 (≥ 4)	exhaustive triple search	enumeration contract; residual gap
Gadget non-existence	$\mathrm{Sp}(4, \mathbb{F}_3)$ sweep	enumeration contract; branch-test replay
Thm. 6	two-copy $\mathrm{Sp}(4, \mathbb{F}_3)$ sweep	enumeration contract; gate-sequence replay
Prop. 5 ($\|\mathrm{S}\rangle$ rigidity)	analytic proof	—
$\|\mathbb{N}\rangle^{\otimes 4} \leq 7$ (App. C.3.3)	SA decomposition	numerical; SymPy [MSP$^+$17]; Lean 4
$\chi(\|H\rangle^{\otimes 4}) \geq 4$ [BSS16]	exhaustive triple search (verification only)	enumeration contract; residual gap
$\chi(\|T\rangle^{\otimes 2}) \leq 2$	SA decomposition	numerical
$\chi(\|T\rangle^{\otimes 3}) \leq 3$	SA decomposition	numerical
$\chi(\|T\rangle^{\otimes 4}) = 3$	algebraic identity (App. C.4)	numerical

Table 3: Result-to-artifact-to-verifier map for the paper's key claims, indicating the primary search method and validation channels (numerical, exact-rational, and Lean 4 machine-checking).

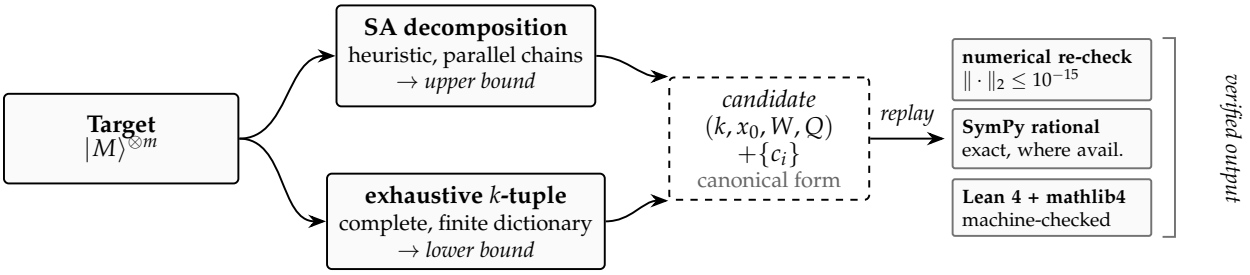

Figure 1: The `stabrank` decomposition pipeline (upper-bound side). Simulated annealing returns a candidate canonical-form decomposition (k, x_0, W, Q) with coefficients $\{c_i\}$, replayed through three independent verifiers: numerical at machine precision (all seven qutrit identities), exact-rational in SymPy [MSP$^+$17] (the heaviest identity, $|\mathbb{N}\rangle^{\otimes 4}$), and Lean 4 + mathlib4 (all seven qutrit identities). The exhaustive k-tuple enumeration and the symplectic-quotient sweep (Section 3) instead emit JSON certificates audited via the path in Section 4.

The Lean 4 formalizations re-derive the canonical-form amplitude identities from the parameters of Appendix C alone, with no dependency on the search or its floating-point residual. Soundness of the exhaustive certificates rests on a large residual gap: across every published certificate the smallest non-witness least-squares residual is ≈ 0.14, nine orders of magnitude above the 10^{-10} tolerance used to flag a true witness. The $\mathrm{Sp}(4, \mathbb{F}_3)$ gadget sweep uses `atol` $= 10^{-8}$ for proportionality-to-unitary and `atol` $= 10^{-5}$ for Clifford-equivalence against the 216-element single-qutrit Clifford group; recovering the T_3 injection gadget as a positive control confirms calibration.

5 Conclusions

We give the first nontrivial exact-rank upper-bound exponents for the three non-T_3 qutrit orbits ($\gamma_{\mathbb{S}} \leq \log_3(2)/2$, $\gamma_{H_3}, \gamma_{\mathbb{N}} \leq \log_3(4)/3$, all strictly below the $\gamma_{T_3} \leq 1/2$ baseline of [KS21]), exhaustive small-m tight values $\chi(|M\rangle^{\otimes 3}) = 4$ for $|M\rangle \in \{|\mathbb{S}\rangle, |H_3\rangle, |\mathbb{N}\rangle\}$, and the first $\Omega(m/\log m)$ asymptotic lower bounds for $|H_3\rangle$ and $|\mathbb{N}\rangle$ via a qutrit adaptation of [LS22]. Operationally, $|H_3\rangle$ and $|\mathbb{N}\rangle$ admit explicit two-copy probabilistic conversion to injectable phase states. In contrast, $|\mathbb{S}\rangle$ is rigid: exhaustive searches over the 2-qutrit and 3-qutrit symplectic groups (using pruning) confirm that no conversion protocol exists. Thus, the smaller upper-bound exponent of $|\mathbb{S}\rangle$ remains operationally inaccessible under low-copy consumption.

An interesting open direction is to establish asymptotic lower bounds for $|\mathbb{S}\rangle$, where the subset-sum obstruction technique used for the other qutrit orbits does not directly apply. Standard stabilizer-nullity or dyadic-monotone techniques (e.g., following [BCHK20]) might offer a starting point, though their applicability to $|\mathbb{S}\rangle$ remains to be fully explored. Similarly, while approximate stabilizer rank lower bounds have been studied in the qubit setting (such as the probabilistic bounds in [MT23]), extending these results to the qutrit setting is another potential avenue of inquiry. Finally, it remains an open question whether a physical Clifford conversion protocol for $|\mathbb{S}\rangle$ is possible for any number of copies, or if the stabilizer rank exponent can be made operationally useful via alternative consumption models [RB01, Hal07, BKM21, MBH22].

Acknowledgements

We thank David Gosset for an early look at the manuscript. We used the generative AI tool Claude Opus 4.7 during code development for the `stabrank` library, including the Lean 4 + mathlib4 formalizations of the qutrit decomposition identities of Appendix C. This work was supported by the U.S. Department of Energy, Office of Science, Office of Advanced Scientific Computing Research, Accelerated Research in Quantum Computing under Award Number DE-SC0025336. This material is also based upon work supported by the U.S. Department of Energy, Office of Science, National Quantum Information Science Research Centers, Quantum Science Center. FL acknowledges support from the European Union through the QLASS project (EU Horizon Europe grant agreement 101135876). Views and opinions expressed are however those of the authors only and do not necessarily reflect those of the European Union. Neither the European Union nor the granting authority can be held responsible for them.

References

[ACB12] Hussain Anwar, Earl T. Campbell, and Dan E. Browne. Qutrit magic state distillation. *New J. Phys.*, 14:063006, 2012.

[AG04] Scott Aaronson and Daniel Gottesman. Improved simulation of stabilizer circuits. *Phys. Rev. A*, 70:052328, 2004.

[App05] D. M. Appleby. Symmetric informationally complete-positive operator valued measures and the extended Clifford group. *J. Math. Phys.*, 46:052107, 2005.

[BBC+19] Sergey Bravyi, Dan Browne, Padraic Calpin, Earl Campbell, David Gosset, and Mark Howard. Simulation of quantum circuits by low-rank stabilizer decompositions. *Quantum*, 3:181, 2019.

[BCHK20] Michael Beverland, Earl Campbell, Mark Howard, and Vadym Kliuchnikov. Lower bounds on the non-Clifford resources for quantum computations. *Quantum Sci. Technol.*, 5:035009, 2020.

[BG16] Sergey Bravyi and David Gosset. Improved classical simulation of quantum circuits dominated by Clifford gates. *Phys. Rev. Lett.*, 116:250501, 2016.

[BK05] Sergey Bravyi and Alexei Kitaev. Universal quantum computation with ideal Clifford gates and noisy ancillas. *Phys. Rev. A*, 71:022316, 2005.

[BKM21] Robert I. Booth, Aleks Kissinger, and Damian Markham. Outcome determinism in measurement-based quantum computation with qudits, 2021.

[BSS16] Sergey Bravyi, Graeme Smith, and John A. Smolin. Trading classical and quantum computational resources. *Phys. Rev. X*, 6:021043, 2016.

[CAB12] Earl T. Campbell, Hussain Anwar, and Dan E. Browne. Magic-state distillation in all prime dimensions using quantum Reed–Muller codes. *Phys. Rev. X*, 2:041021, 2012.

[CGK17] Shawn X. Cui, Daniel Gottesman, and Anirudh Krishna. Diagonal gates in the Clifford hierarchy. *Phys. Rev. A*, 95:012329, 2017.

[DH15] Hillary Dawkins and Mark Howard. Qutrit magic state distillation tight in some directions. *Phys. Rev. Lett.*, 115:030501, 2015.

[dMU21] Leonardo de Moura and Sebastian Ullrich. The Lean 4 theorem prover and programming language. In *Automated Deduction – CADE 28*, pages 625–635, 2021.

[Got98] Daniel Gottesman. The Heisenberg representation of quantum computers, 1998.

[Got99] Daniel Gottesman. Fault-tolerant quantum computation with higher-dimensional systems. *Chaos, Solitons & Fractals*, 10:1749–1758, 1999.

[Hal07] William Hall. Cluster state quantum computation for many-level systems. *Phys. Rev. A*, 75:062321, 2007.

[HDDM05] Erik Hostens, Jeroen Dehaene, and Bart De Moor. Stabilizer states and Clifford operations for systems of arbitrary dimensions and modular arithmetic. *Phys. Rev. A*, 71:042315, 2005.

[HG19] Markus Heinrich and David Gross. Robustness of magic and symmetries of the stabiliser polytope. *Quantum*, 3:132, 2019.

[HL19] Yifei Huang and Peter Love. Approximate stabilizer rank and improved weak simulation of Clifford-dominated circuits for qudits. *Phys. Rev. A*, 99:052307, 2019.

[HV12] Mark Howard and Jiri Vala. Qudit versions of the qubit $\pi/8$ gate. *Phys. Rev. A*, 86:022316, 2012.

[HWVE14] Mark Howard, Joel Wallman, Victor Veitch, and Joseph Emerson. Contextuality supplies the 'magic' for quantum computation. *Nature*, 510:351–355, 2014.

[JP20] Akalank Jain and Shiroman Prakash. Qutrit and ququint magic states. *Phys. Rev. A*, 102:042409, 2020.

[KS21] Lucas Kocia and Mohan Sarovar. Improved simulation of quantum circuits by fewer Gaussian eliminations. *Phys. Rev. A*, 103:022603, 2021.

[KS25] Amolak Ratan Kalra and Pulkit Sinha. Stabilizer ranks, Barnes-Wall lattices and magic monotones, 2025.

[Lab22] Farrokh Labib. Stabilizer rank and higher-order Fourier analysis. *Quantum*, 6:645, 2022.

[LR26] Farrokh Labib and Vincent Russo. `stabrank`: a library for stabilizer-rank decompositions and certificates. `https://github.com/unitaryfoundation/stabrank`, 2026.

[LS22] Benjamin Lovitz and Vincent Steffan. New techniques for bounding stabilizer rank. *Quantum*, 6:692, 2022.

[MBH22] Jelena Mackeprang, Daniel Bhatti, and Matty J. Hoban. The power of qutrits for non-adaptive measurement-based quantum computing, 2022.

[MSP+17] Aaron Meurer, Christopher P. Smith, Mateusz Paprocki, Ondřej Čertík, Sergey B. Kirpichev, Matthew Rocklin, Amit Kumar, Sergiu Ivanov, Jason K. Moore, Sartaj Singh, Thilina Rathnayake, Sean Vig, Brian E. Granger, Richard P. Muller, Francesco Bonazzi, Harsh Gupta, Shivam Vats, Fredrik Johansson, Fabian Pedregosa, Matthew J. Curry, Andy R. Terrel, Štěpán Roučka, Ashutosh Saboo, Isuru Fernando, Sumith Kulal, Robert Cimrman, and Anthony Scopatz. SymPy: Symbolic computing in Python. *PeerJ Computer Science*, 3:e103, 2017.

[MT23] Saeed Mehraban and Mehrdad Tahmasbi. Quadratic lower bounds on the approximate stabilizer rank: A probabilistic approach, 2023.

[PG20] Shiroman Prakash and Aashi Gupta. Contextual bound states for qudit magic state distillation. *Phys. Rev. A*, 101:010303, 2020.

[Pra20] Shiroman Prakash. Magic state distillation with the ternary Golay code. *Proc. R. Soc. A*, 476:20200187, 2020.

[PSV22] Shir Peleg, Amir Shpilka, and Ben Lee Volk. Lower bounds on stabilizer rank. *Quantum*, 6:652, 2022.

[Qas20] Hammam Qassim. *Classical Simulations of Quantum Systems Using Stabilizer Decompositions*. PhD thesis, University of Waterloo, 2020.

[QPG21] Hammam Qassim, Hakop Pashayan, and David Gosset. Improved upper bounds on the stabilizer rank of magic states. *Quantum*, 5:606, 2021.

[RB01] Robert Raussendorf and Hans J. Briegel. A one-way quantum computer. *Phys. Rev. Lett.*, 86:5188–5191, 2001.

[The20] The mathlib Community. The Lean mathematical library. In *Proceedings of the 9th ACM SIGPLAN International Conference on Certified Programs and Proofs*, CPP 2020, pages 367–381, 2020.

[VFGE12] Victor Veitch, Christopher Ferrie, David Gross, and Joseph Emerson. Negative quasi-probability as a resource for quantum computation. *New J. Phys.*, 14:113011, 2012.

[VMGE14] Victor Veitch, S. A. Hamed Mousavian, Daniel Gottesman, and Joseph Emerson. The resource theory of stabilizer quantum computation. *New J. Phys.*, 16:013009, 2014.

[Zhu10] Huangjun Zhu. SIC POVMs and Clifford groups in prime dimensions. *J. Phys. A: Math. Theor.*, 43:305305, 2010.

A Symplectic-quotient reduction

Reduction of the search domain $\mathrm{Cl}(2,3) = H(2,3) \rtimes \mathrm{Sp}(4,\mathbb{F}_3)$ to its symplectic quotient, used in the gadget non-existence result and Theorem 6. For an entangling two-qutrit Clifford $C \in \mathrm{Cl}(2,3)$ and ancilla outcome $k \in \mathbb{F}_3$, write

$$E_k(C,|M\rangle) = (\mathbb{1}_{\mathrm{data}} \otimes \langle k|_{\mathrm{anc}})C(\mathbb{1}_{\mathrm{data}} \otimes |M\rangle) \in \mathcal{L}(\mathbb{C}^3) \tag{20}$$

for the unnormalized data-register linear operator implemented on measurement branch k. In the two-copy conversion case of Theorem 6 the data register is also prepared in $|M\rangle$, so the branch-k data-register output state is the vector $E_k(C,|M\rangle)|M\rangle \in \mathbb{C}^3$.

Lemma 7. *Fix $|M\rangle \in \mathbb{C}^3$ and write $C_{\mathrm{ent}} = DC_{\mathrm{sp}}$ with $D \in H(2,3)$ and $C_{\mathrm{sp}} \in \mathrm{Sp}(4,\mathbb{F}_3)$. Decompose D into its data-leg and ancilla-leg factors $D = D_{\mathrm{data}} \otimes D_{\mathrm{anc}}$, with $D_{\mathrm{anc}} = X^a Z^b$ for some $(a,b) \in \mathbb{F}_3^2$. Then for every $k \in \mathbb{F}_3$,*

$$E_k(C_{\mathrm{ent}},|M\rangle) = \omega_3^{b(k-a)} D_{\mathrm{data}} E_{k-a}(C_{\mathrm{sp}},|M\rangle). \tag{21}$$

Consequently, the existence of a valid deterministic injection gadget for $|M\rangle$ depends only on the $\mathrm{Sp}(4,\mathbb{F}_3)$ coset of C_{ent}; the same applies to the existence of a valid two-copy conversion protocol in the sense of Section 3.1.

Proof. Using the identity $\langle k|X^aZ^b = \omega_3^{b(k-a)}\langle k-a|$,

$$\begin{aligned} E_k(C_{\mathrm{ent}},|M\rangle) &= \langle k|_{\mathrm{anc}}(D_{\mathrm{data}} \otimes D_{\mathrm{anc}})C_{\mathrm{sp}}(\mathbb{1} \otimes |M\rangle) \\ &= D_{\mathrm{data}}(\langle k|D_{\mathrm{anc}})_{\mathrm{anc}}C_{\mathrm{sp}}(\mathbb{1} \otimes |M\rangle) \\ &= \omega_3^{b(k-a)} D_{\mathrm{data}} E_{k-a}(C_{\mathrm{sp}},|M\rangle). \end{aligned} \tag{22}$$

The prefactor D_{data} is a single-qutrit Pauli, and $k \mapsto k-a$ permutes $\mathbb{F}_3$, so the multisets $\{E_k(C_{\mathrm{ent}},M)\}_k$ and $\{E_k(C_{\mathrm{sp}},M)\}_k$ coincide up to a global Pauli prefactor and branch-dependent phases. Proportionality to a unitary, the Clifford-byproduct condition, and the Clifford-equivalent-to-phase-state condition are all invariant under both transformations. □

The reduction shows that whether a valid gadget exists is a property of the $\mathrm{Sp}(4,\mathbb{F}_3)$ coset, not of any particular representative. It does not say anything about gate count: the circuits in (15) are the symplectic representatives returned by the search, and a different coset representative might admit a shorter decomposition.

B Proof of Proposition 5

Proof of Proposition 5. For (i), $\mathrm{Cl}(1,3)$ is generated by the qutrit Pauli operators X (shift: $X|j\rangle = |j+1\rangle$) and Z (clock: $Z|j\rangle = \omega^j|j\rangle$), the phase gate $S = \mathrm{diag}(1,1,\omega)$, and the qutrit Hadamard $H_{jk} = \omega^{jk}/\sqrt{3}$. Any $|\phi\rangle \in \mathcal{O}_S$ has the form $|\phi_{a,b,c}\rangle = (|a\rangle - \omega^c|b\rangle)/\sqrt{2}$ for some two-element support $\{a,b\} \subset \mathbb{F}_3$ with $a \neq b$ and some phase exponent $c \in \mathbb{F}_3$; this pattern is preserved by each generator on every such state:

- X sends $|\phi_{a,b,c}\rangle$ to $|\phi_{a+1,b+1,c}\rangle$.
- Z sends $|\phi_{a,b,c}\rangle$ to $\omega^a|\phi_{a,b,c+(b-a)}\rangle$.
- S acts trivially on $|j\rangle$ for $j \in \{0,1\}$ and as ω on $|2\rangle$; it sends $|\phi_{a,b,c}\rangle$ to $|\phi_{a,b,c+[b=2]-[a=2]}\rangle$.
- H sends $|\phi_{a,b,c}\rangle$ to

$$H|\phi_{a,b,c}\rangle = \frac{1}{\sqrt{6}} \sum_{j\in\mathbb{F}_3} \left(\omega^{aj} - \omega^{c+bj}\right)|j\rangle.$$

  The coefficient at $|j\rangle$ vanishes iff $(a-b)j \equiv c \pmod 3$, which has a unique solution $j^* \in \mathbb{F}_3$ since $a \neq b$. For the other two indices j_1, j_2, factor each coefficient as $\omega^{aj}(1-\omega^{k_j})$ with $k_j = c + (b-a)j$; then k_{j_1} and k_{j_2} take the values 1 and 2 in some order. Since $|1-\omega| = |1-\omega^2| = \sqrt{3}$, the two nonzero amplitudes each have modulus $1/\sqrt{2}$, and their ratio takes the form $-\omega^{c'}$ for some $c' \in \mathbb{F}_3$ (using $(1-\omega^2)/(1-\omega) = -\omega^2$). Therefore $H|\phi_{a,b,c}\rangle$ is, up to a global phase, $|\phi_{j_1,j_2,c'}\rangle$.

The pattern is thus closed under the generators and so under all of $\mathrm{Cl}(1,3)$.

For (ii), the three-parameter family $\{|\phi_{a,b,c}\rangle\}$ has at most $\binom{3}{2} \times 3 = 9$ projective elements (three unordered 2-element supports, three phase exponents $c \in \mathbb{F}_3$ each). The X-action shows all three supports are reached from $|\mathbb{S}\rangle = |\phi_{1,2,0}\rangle$, and on a fixed support the three values of c give projectively distinct states: $|\phi_{a,b,c}\rangle$ and $|\phi_{a,b,c'}\rangle$ are projectively equal iff $\omega^c = \omega^{c'}$ (the ratio of the $|b\rangle$ amplitudes), iff $c = c'$ in $\mathbb{F}_3$. Hence $|\mathcal{O}_S| = 9$ and $|\mathrm{Stab}(|\mathbb{S}\rangle)| = 216/9 = 24$ by orbit-stabilizer.

The final claim is immediate from (i): a state with support cardinality 2 and equal-modulus nonzero amplitudes cannot have two amplitudes of differing moduli, so the $|a_i|/|a_j| \geq 2$ hypothesis of Proposition 4 fails for every $|\phi\rangle \in \mathcal{O}_S$. Since the stabilizer rank is invariant under the single-qutrit Clifford action, testing the hypothesis on $\mathcal{O}_S$ exhausts the freedom available, and Proposition 4 yields no $\chi(|\mathbb{S}\rangle^{\otimes m})$ lower bound. □

C Explicit stabilizer decompositions

This appendix groups the explicit stabilizer decompositions by orbit. Each verification states the canonical-form data $(k_i, x_{0,i}, W_i, Q_i)$ for the basis stabilizer states $|\sigma_i\rangle$ via (1), gives linear coefficients α_i, and supplies an algebraic proof that $\sum_i \alpha_i|\sigma_i\rangle$ equals the target $|\psi\rangle$. The verifications all follow a common pattern: a particular feature of the target (its support partition for Strange, its product factorization $|H_3\rangle = (N/2)(|0\rangle + |+\rangle)$ for H_3, the Norrell-character form $|\mathbb{N}\rangle = (1/\sqrt{6})\sum_y c_N(y)|y\rangle$ for Norrell) reduces the 3^m component identities to a small set of scalar identities in the orbit-specific algebraic constants. The underlying decompositions were originally produced by the simulated-annealing search of the `stabrank` library (Section 4). Every qutrit decomposition theorem in this appendix is also formalized in Lean 4 + mathlib4 in the accompanying `LeanProofs/` directory; the specific Lean file(s) realizing each proof are named at the end of the corresponding proof. The qubit T-type $\chi(|T\rangle^{\otimes 4}) \leq 3$ decomposition of Appendix C.4 is verified numerically at machine precision and is not (yet) Lean-formalized.

Throughout the appendix $\omega = e^{2\pi i/3}$ denotes the primitive cube root of unity, satisfying

$$1 + \omega + \omega^2 = 0, \qquad \omega = -\frac{1}{2} + \frac{i\sqrt{3}}{2}, \qquad \omega^2 = -\frac{1}{2} - \frac{i\sqrt{3}}{2}, \tag{23}$$

and $\bar{\cdot}$ denotes entrywise complex conjugation in the computational basis. The constants c, N for H_3, the Norrell character c_N, and the twelfth-root ξ used in the Norrell $m = 4$ proof are introduced at the head of each orbit subsection.

C.1 Strange-orbit decompositions

C.1.1 $\chi(|\mathbb{S}\rangle^{\otimes 2}) = 2$

Proof of Theorem 2. Fix two quadratic forms on $\mathbb{F}_3^2$,

$$Q_1(y) = y_0^2 + y_0y_1 + y_1^2, \qquad Q_2(y) = y_0^2 + 2y_0y_1 + y_1^2 \pmod 3, \tag{24}$$

and let $|\sigma_j\rangle$ be the two-qutrit stabilizer state given by the canonical form (1) with $k = 2$, $x_0 = 0$, $W = I_2$, and quadratic phase polynomial Q_j,

$$|\sigma_j\rangle = \frac{1}{3}\sum_{y\in\mathbb{F}_3^2} \omega^{Q_j(y)}|y\rangle. \tag{25}$$

Subtracting the two states,

$$|\sigma_1\rangle - |\sigma_2\rangle = \frac{1}{3}\sum_{y\in\mathbb{F}_3^2} \omega^{y_0^2+y_1^2}\big(\omega^{y_0y_1} - \omega^{2y_0y_1}\big)|y\rangle. \tag{26}$$

Substituting $\omega = -\frac{1}{2} + \frac{i\sqrt{3}}{2}$ gives $\omega^a - \omega^{2a} = 0, +i\sqrt{3}, -i\sqrt{3}$ for $a \equiv 0, 1, 2 \pmod 3$, so the inner bracket in (26) vanishes whenever $y_0 = 0$ or $y_1 = 0$. On the four remaining $y \in \{1,2\}^2$ one has $y_0^2 + y_1^2 \equiv 2 \pmod 3$ uniformly, $y_0y_1 \equiv 1$ at $(1,1), (2,2)$, and $y_0y_1 \equiv 2$ at $(1,2), (2,1)$, so

$$|\sigma_1\rangle - |\sigma_2\rangle = \frac{i\sqrt{3}}{3}\omega^2\big(|11\rangle - |12\rangle - |21\rangle + |22\rangle\big) = \frac{2i\sqrt{3}}{3}\omega^2|\mathbb{S}\rangle^{\otimes 2}, \tag{27}$$

where the second equality uses $|\mathbb{S}\rangle^{\otimes 2} = \frac{1}{2}(|1\rangle - |2\rangle)^{\otimes 2} = \frac{1}{2}(|11\rangle - |12\rangle - |21\rangle + |22\rangle)$. Inverting (27) (and using $\omega^{-2} = \omega$, $i^{-1} = -i$),

$$|\mathbb{S}\rangle^{\otimes 2} = -\frac{i\sqrt{3}}{2}\omega\big(|\sigma_1\rangle - |\sigma_2\rangle\big), \tag{28}$$

matching Theorem 2. This exhibits $|\mathbb{S}\rangle^{\otimes 2}$ as a $\mathbb{C}$-linear combination of two stabilizer states, so $\chi(|\mathbb{S}\rangle^{\otimes 2}) \le 2$.

For the lower bound, $|\mathbb{S}\rangle^{\otimes 2}$ has computational-basis support $\{(1,1),(1,2),(2,1),(2,2)\}$, of cardinality four. Any single 2-qutrit stabilizer state has, by (1), support contained in an affine subspace $x_0 + W\mathbb{F}_3^k \subseteq \mathbb{F}_3^2$, hence of cardinality 3^r for some $r \in \{0,1,2\}$. Since $4 \notin \{1,3,9\}$, $|\mathbb{S}\rangle^{\otimes 2}$ is not proportional to any stabilizer state, and $\chi(|\mathbb{S}\rangle^{\otimes 2}) \neq 1$. Combining, $\chi(|\mathbb{S}\rangle^{\otimes 2}) = 2$.

Machine-checked Lean formalization: `StrangeM2Pointwise.lean`. □

C.1.2 $\chi(|\mathbb{S}\rangle^{\otimes 3}) \le 4$

Proof that $\chi(|\mathbb{S}\rangle^{\otimes 3}) \le 4$. Set $W = (e_0, e_2) \in \mathbb{F}_3^{3\times 2}$. Define four 3-qutrit stabilizer states by (1), all with $k = 2$ and the matrix W above:

$$\begin{aligned}
&|\sigma_1\rangle : x_0 = (0,2,0), Q_1(w) = w_0^2 + w_0w_1 \pmod 3,\\
&|\sigma_3\rangle : x_0 = (0,2,0), Q_3(w) = w_0^2 + 2w_0w_1 \pmod 3,\\
&|\sigma_2\rangle : x_0 = (0,1,0), Q_2(w) = 2w_0^2 + w_0w_1 + w_1^2 \pmod 3,\\
&|\sigma_4\rangle : x_0 = (0,1,0), Q_4(w) = 2w_0^2 + 2w_0w_1 + w_1^2 \pmod 3.
\end{aligned} \tag{29}$$

Set $\alpha = \frac{\sqrt{6}}{4}e^{-i\pi/6} = \frac{3\sqrt{2}-i\sqrt{6}}{8}$ and $\beta = -\frac{i\sqrt{6}}{4}$. We claim

$$|\mathrm{S}\rangle^{\otimes 3} = \alpha\big(|\sigma_1\rangle - |\sigma_3\rangle\big) + \beta\big(|\sigma_2\rangle - |\sigma_4\rangle\big). \tag{30}$$

Since $|\mathrm{S}\rangle = (|1\rangle - |2\rangle)/\sqrt{2}$, the amplitude $[|\mathrm{S}\rangle^{\otimes 3}]_y$ vanishes whenever some $y_i = 0$, and equals $(-1)^{n_2}/(2\sqrt{2})$ at $y \in \{1,2\}^3$, where $n_2 = |\{i : y_i = 2\}|$. The shared W sends $w \mapsto (w_0, 0, w_1)$, so $|\sigma_1\rangle, |\sigma_3\rangle$ have support on the plane $\{y : y_1 = 2\}$ and $|\sigma_2\rangle, |\sigma_4\rangle$ on $\{y : y_1 = 1\}$; both sides of (30) vanish on the remaining plane $y_1 = 0$, so the identity decouples into two independent verifications.

Consider the plane $y_1 = 2$. On this plane the canonical-form parameter $w = (w_0, w_1)$ satisfies $w_0 = y_0$ and $w_1 = y_2$, so $[\sigma_j]_y = \omega^{Q_j(y_0,y_2)}/3$ for $j \in \{1,3\}$. The polynomials Q_1, Q_3 differ only in the cross-term $\pm w_0 w_1 = \pm y_0 y_2$, which vanishes whenever $y_0 = 0$ or $y_2 = 0$; on those lines $|\sigma_1\rangle_y = |\sigma_3\rangle_y$, so $\alpha(|\sigma_1\rangle - |\sigma_3\rangle)_y = 0$, matching $|\mathrm{S}\rangle_y^{\otimes 3} = 0$. At $(y_0, y_2) \in \{1,2\}^2$ one has $y_0^2 \equiv 1 \pmod 3$, and direct evaluation yields

$$(Q_1, Q_3)(y_0, y_2) = \begin{cases} (2,0), & y_0 = y_2, \\ (0,2), & y_0 \neq y_2, \end{cases} \qquad \text{whence} \qquad \omega^{Q_1} - \omega^{Q_3} = \epsilon(y_0, y_2)(\omega^2 - 1), \tag{31}$$

with $\epsilon(y_0, y_2) = (-1)^{[y_0=2]+[y_2=2]}$ equal to $+1$ when $y_0 = y_2$ and -1 otherwise. Meanwhile $[|\mathrm{S}\rangle^{\otimes 3}]_{(y_0,2,y_2)} = -\epsilon(y_0, y_2)/(2\sqrt{2})$ (the leading minus sign coming from the fixed $y_1 = 2$ factor). The four-point identity therefore reduces to the single scalar equation $\alpha(\omega^2 - 1)/3 = -1/(2\sqrt{2})$. Using $\omega^2 - 1 = -\frac{3}{2} - \frac{i\sqrt{3}}{2} = -\sqrt{3}e^{i\pi/6}$,

$$\alpha = \frac{-3}{2\sqrt{2}(-\sqrt{3}e^{i\pi/6})} = \frac{3}{2\sqrt{6}}e^{-i\pi/6} = \frac{\sqrt{6}}{4}e^{-i\pi/6}, \tag{32}$$

which matches the stated value of α.

Consider the plane $y_1 = 1$. The same argument applies: Q_2 and Q_4 agree whenever $y_0 = 0$ or $y_2 = 0$, so $\beta(|\sigma_2\rangle - |\sigma_4\rangle)$ vanishes there. At $(y_0, y_2) \in \{1,2\}^2$, $y_0^2 \equiv y_2^2 \equiv 1$ reduces $Q_2 \equiv y_0 y_2$ and $Q_4 \equiv 2y_0 y_2 \pmod 3$, giving

$$(Q_2, Q_4)(y_0, y_2) = \begin{cases} (1,2), & y_0 = y_2, \\ (2,1), & y_0 \neq y_2, \end{cases} \quad \text{whence} \quad \omega^{Q_2} - \omega^{Q_4} = i\sqrt{3}\epsilon(y_0, y_2). \tag{33}$$

Now $[|\mathrm{S}\rangle^{\otimes 3}]_{(y_0,1,y_2)} = \epsilon(y_0, y_2)/(2\sqrt{2})$, so the identity reduces to $\beta i\sqrt{3}/3 = 1/(2\sqrt{2})$, giving

$$\beta = \frac{3}{2\sqrt{2}i\sqrt{3}} = -\frac{i\sqrt{6}}{4}, \tag{34}$$

which matches the stated value of β.

Machine-checked Lean formalization: `StrangeM3.lean`, `StrangeM3Pointwise.lean`. □

C.2 H_3-orbit decompositions

Throughout this subsection let $c = (\sqrt{3} - 1)/2$ and $N = \sqrt{3 - \sqrt{3}}$. Direct verification gives

$$|H_3\rangle = \frac{N}{2}\big(|0\rangle + |+\rangle\big), \qquad |+\rangle = \frac{1}{\sqrt{3}}\big(|0\rangle + |1\rangle + |2\rangle\big), \tag{35}$$

both equations $N^2(1+1/\sqrt{3})/2 = 1$ and $N^2/(2\sqrt{3}) = c$ reducing to $N^2 = 3-\sqrt{3}$. We will use the algebraic identities

$$c(c+1) = \frac{1}{2}, \qquad c(\sqrt{3}+1) = 1, \qquad \sqrt{3}-1 = 2c, \tag{36}$$

together with $1/N^3 = (3+\sqrt{3})/(6N)$; all are immediate from $c = (\sqrt{3}-1)/2$ and $N^2 = 3-\sqrt{3}$.

C.2.1 $\chi(|H_3\rangle^{\otimes 2}) \le 3$

Proof that $\chi(|H_3\rangle^{\otimes 2}) \le 3$. Define three 2-qutrit stabilizer states by (1):

$$\begin{aligned} &|\sigma_1\rangle : k=1, x_0=0, W=e_1, Q_1=0, \quad \text{so } |\sigma_1\rangle = |0,+\rangle, \\ &|\sigma_2\rangle : k=1, x_0=0, W=e_0, Q_2=0, \quad \text{so } |\sigma_2\rangle = |+,0\rangle, \\ &|\sigma_3\rangle : k=2, x_0=0, W=I_2, Q_3(y) = 2y_0^2 + y_1^2 \pmod 3, \end{aligned} \tag{37}$$

and set

$$\alpha_1 = \frac{c\sqrt{3}}{N^2}(1-c\omega), \qquad \alpha_2 = \frac{c\sqrt{3}}{N^2}(1-c\omega^2), \qquad \alpha_3 = \frac{3c^2}{N^2}. \tag{38}$$

We claim

$$|H_3\rangle^{\otimes 2} = \alpha_1|\sigma_1\rangle + \alpha_2|\sigma_2\rangle + \alpha_3|\sigma_3\rangle. \tag{39}$$

By (35), $[|H_3\rangle^{\otimes 2}]_y = c^{|y|_*}/N^2$ with $|y|_* = [y_0 \neq 0] + [y_1 \neq 0]$. The components $[\sigma_1]_y = (1/\sqrt{3})[y_0 = 0]$, $[\sigma_2]_y = (1/\sqrt{3})[y_1 = 0]$, and $[\sigma_3]_y = \omega^{Q_3(y)}/3$ all depend on y only through the pair $(a,b) = ([y_0 \neq 0],[y_1 \neq 0]) \in \{0,1\}^2$, since $y_i^2 \equiv [y_i \neq 0] \pmod 3$. In particular $Q_3(y) \equiv 2a+b \pmod 3$, and (39) reduces to four scalar identities, one per class.

Writing $\alpha_1/\sqrt{3} = (c/N^2)(1-c\omega)$ and $\alpha_2/\sqrt{3} = (c/N^2)(1-c\omega^2)$, the right side of (39) at any y in class (a,b) equals

$$[\alpha_1\sigma_1]_y + [\alpha_2\sigma_2]_y + [\alpha_3\sigma_3]_y = \frac{c}{N^2}[a=0](1-c\omega) + \frac{c}{N^2}[b=0](1-c\omega^2) + \frac{c^2}{N^2}\omega^{2a+b}. \tag{40}$$

Evaluating (40) in each class (using $\omega+\omega^2 = -1$ and $c(1+c) = 1/2$):

(a,b)	RHS	target c^{a+b}/N^2
$(0,0)$	$\frac{c}{N^2}\left[(1-c\omega)+(1-c\omega^2)\right] + \frac{c^2}{N^2} = \frac{2c(1+c)}{N^2} = \frac{1}{N^2}$	$\frac{1}{N^2}$
$(0,1)$	$\frac{c}{N^2}(1-c\omega) + \frac{c^2}{N^2}\omega = \frac{c}{N^2}$	$\frac{c}{N^2}$
$(1,0)$	$\frac{c}{N^2}(1-c\omega^2) + \frac{c^2}{N^2}\omega^2 = \frac{c}{N^2}$	$\frac{c}{N^2}$
$(1,1)$	$\frac{c^2}{N^2}\omega^0 = \frac{c^2}{N^2}$	$\frac{c^2}{N^2}$

This establishes (39) and hence $\chi(|H_3\rangle^{\otimes 2}) \le 3$.

Machine-checked Lean formalization: `H3M2Pointwise.lean`. □

C.2.2 $\chi(|H_3\rangle^{\otimes 3}) \le 4$

Proof that $\chi(|H_3\rangle^{\otimes 3}) \le 4$. Define four 3-qutrit stabilizer states by (1): $|\sigma_j\rangle$ for $j \in \{1,2\}$ has $k = 3$, $x_0 = 0$, $W = I_3$, and $Q_j(y) \pmod 3$ given by

$$Q_1(y) = 2y_0^2 + 2y_1^2 + y_2^2, \qquad Q_2(y) = y_0^2 + y_1^2 + 2y_2^2, \tag{41}$$

and

$$|\sigma_3\rangle = |0,0,+\rangle, \qquad |\sigma_4\rangle = |+,+,0\rangle, \tag{42}$$

recognizing the canonical form with $k = 1$, $W = e_2$, $Q_3 = 0$ and $k = 2$, $W = (e_0, e_1)$, $Q_4 = 0$ respectively. Set

$$\alpha_1 = \frac{3c}{4N}(1+i), \quad \alpha_2 = \frac{3c}{4N}(1-i), \quad \alpha_3 = \alpha_4 = \frac{3}{4N}. \tag{43}$$

We claim

$$|H_3\rangle^{\otimes 3} = \alpha_1|\sigma_1\rangle + \alpha_2|\sigma_2\rangle + \alpha_3|\sigma_3\rangle + \alpha_4|\sigma_4\rangle. \tag{44}$$

Both Q_1 and Q_2 depend on y only through $y_i^2 \pmod 3 = [y_i \neq 0]$, and (42) likewise depends only on which coordinates of y vanish, so each component of the right side of (44) depends only on the pair

$$(n,z) = \big(|\{i \in \{0,1\} : y_i \neq 0\}|, [y_2 \neq 0]\big) \in \{0,1,2\} \times \{0,1\}. \tag{45}$$

Each component of $|H_3\rangle^{\otimes 3}$ depends only on $|y|_* = n + z$ via (35), namely $[|H_3\rangle^{\otimes 3}]_y = c^{n+z}/N^3$. Hence (44) reduces to six scalar identities, one per class.

For the $|\sigma_1\rangle, |\sigma_2\rangle$ contribution at y in class (n,z), the canonical form gives $\alpha_1[\sigma_1]_y + \alpha_2[\sigma_2]_y = (3\sqrt{3})^{-1}(\alpha_1\omega^{2n+z} + \alpha_2\omega^{n+2z})$. Substituting $\omega = -\frac{1}{2} + \frac{i\sqrt{3}}{2}$, the three values of $(\alpha_1\omega^A + \alpha_2\omega^B)$ that arise are

$$\begin{aligned} \alpha_1 + \alpha_2 &= \frac{3c}{2N}, \\ \alpha_1\omega + \alpha_2\omega^2 &= -\frac{3c(1+\sqrt{3})}{4N} = -\frac{3}{4N} \quad (\text{using } c(1+\sqrt{3}) = 1), \\ \alpha_1\omega^2 + \alpha_2\omega &= \frac{3c(\sqrt{3}-1)}{4N} = \frac{3c^2}{2N} \qquad (\text{using } \sqrt{3}-1 = 2c). \end{aligned} \tag{46}$$

Combining with $[\sigma_3]_y = (1/\sqrt{3})[n=0]$ and $[\sigma_4]_y = (1/3)[z=0]$, the right side of (44) at any y in class (n,z) is the entry below; the left side is c^{n+z}/N^3:

(n,z)	$\alpha_1[\sigma_1]_y + \alpha_2[\sigma_2]_y$	$\alpha_3[\sigma_3]_y + \alpha_4[\sigma_4]_y$	RHS at y
$(0,0)$	$\frac{c}{2N\sqrt{3}}$	$\frac{3}{4N}\left(\frac{1}{\sqrt{3}} + \frac{1}{3}\right) = \frac{3+\sqrt{3}}{4N\sqrt{3}}$	$\frac{3+\sqrt{3}}{6N} = 1/N^3$
$(0,1)$	$-\frac{1}{4N\sqrt{3}}$	$\frac{3}{4N\sqrt{3}}$	$\frac{1}{2N\sqrt{3}} = c/N^3$
$(1,0)$	$\frac{c^2}{2N\sqrt{3}}$	$\frac{1}{4N}$	$\frac{1}{2N\sqrt{3}} = c/N^3$
$(1,1)$	$\frac{c}{2N\sqrt{3}}$	0	$\frac{c}{2N\sqrt{3}} = c^2/N^3$
$(2,0)$	$-\frac{1}{4N\sqrt{3}}$	$\frac{1}{4N}$	$\frac{c}{2N\sqrt{3}} = c^2/N^3$
$(2,1)$	$\frac{c^2}{2N\sqrt{3}}$	0	$\frac{c^2}{2N\sqrt{3}} = c^3/N^3$

Equality of the right-hand entries with c^{n+z}/N^3 in each row is the identity

$$\frac{c^k}{N^3} = \frac{c^k(3+\sqrt{3})}{6N}, \qquad k \in \{0,1,2,3\}, \tag{47}$$

which follows from $(3+\sqrt{3})N^2 = (3+\sqrt{3})(3-\sqrt{3}) = 6$. The class-by-class identities then reduce to elementary arithmetic in $c, \sqrt{3}$. As an example, the $(n,z) = (0,0)$ row asks for

$$\frac{c}{2N\sqrt{3}} + \frac{3+\sqrt{3}}{4N\sqrt{3}} = \frac{2c+3+\sqrt{3}}{4N\sqrt{3}} = \frac{(\sqrt{3}-1)+3+\sqrt{3}}{4N\sqrt{3}} = \frac{2+2\sqrt{3}}{4N\sqrt{3}} = \frac{3+\sqrt{3}}{6N} = \frac{1}{N^3}, \tag{48}$$

using $2c = \sqrt{3}-1$ in the third equality and rationalizing $1/\sqrt{3}$ in the fourth. The $(1,0)$ row similarly uses $2c^2 = 2-\sqrt{3}$ to collapse $2c^2+\sqrt{3} = 2$, giving $1/(2N\sqrt{3}) = c/N^3$; the remaining four rows are the analogous one-line manipulations. This proves (44) and hence $\chi(|H_3\rangle^{\otimes 3}) \le 4$.

Machine-checked Lean formalization: `H3M3.lean`, `H3M3Pointwise.lean`. □

C.3 Norrell-orbit decompositions

The single-qutrit Norrell state factors as

$$|\mathbb{N}\rangle = \frac{1}{\sqrt{6}} \sum_{y \in \mathbb{F}_3} c_N(y)|y\rangle, \qquad c_N(0) = c_N(1) = 1, \quad c_N(2) = -2; \tag{49}$$

equivalently $c_N(y) = 1 - 3[y = 2]$. We refer to c_N as the *Norrell character*. The m-fold tensor amplitude is

$$[|\mathbb{N}\rangle^{\otimes m}]_y = \frac{1}{(\sqrt{6})^m} \prod_{i=0}^{m-1} c_N(y_i) = \frac{(-2)^{n_2(y)}}{(\sqrt{6})^m}, \qquad n_2(y) = |\{i : y_i = 2\}|. \tag{50}$$

We will use the polynomial identities

$$y + 2y^2 \equiv [y=2] \pmod 3, \qquad 2y + y^2 \equiv 2[y=2] \pmod 3 \tag{51}$$

on $\mathbb{F}_3$ (verified by direct enumeration), which reduce general quadratic phase polynomials to indicator-only expressions on the supports of the basis stabilizer states.

C.3.1 $\chi(|\mathbb{N}\rangle^{\otimes 2}) \le 3$

Proof that $\chi(|\mathbb{N}\rangle^{\otimes 2}) \le 3$. Define three 2-qutrit stabilizer states by (1):

$$\begin{aligned} &|\sigma_1\rangle : k = 2, x_0 = 0, W = I_2, Q_1(y) = y_0 + y_1 + y_0 y_1 \pmod 3, \\ &|\sigma_2\rangle : k = 0, x_0 = (2,2), \quad \text{so } |\sigma_2\rangle = |2,2\rangle, \\ &|\sigma_3\rangle : k = 2, x_0 = 0, W = I_2, Q_3(y) = 2Q_1(y) \pmod 3, \end{aligned} \tag{52}$$

so $|\sigma_3\rangle = \overline{|\sigma_1\rangle}$ (entrywise complex conjugate in the computational basis). Set $\alpha = -\omega/2$. We claim

$$|\mathbb{N}\rangle^{\otimes 2} = \alpha|\sigma_1\rangle + |\sigma_2\rangle + \overline{\alpha}|\sigma_3\rangle, \tag{53}$$

equivalently $|\mathbb{N}\rangle^{\otimes 2} = -\frac{\omega}{2}|\sigma_1\rangle + |2,2\rangle - \frac{\omega^2}{2}|\sigma_3\rangle$.

The polynomial Q_1 factors as

$$Q_1(y) \equiv (1+y_0)(1+y_1) - 1 \pmod 3, \tag{54}$$

so $Q_1(y) \equiv 2 \pmod 3$ iff $(1+y_0)(1+y_1) \equiv 0$, iff $y_0 = 2$ or $y_1 = 2$. Equivalently,

$$[Q_1(y) = 2] = [y_0 = 2] + [y_1 = 2] - [y_0 = y_1 = 2]. \tag{55}$$

By (1), the contribution of $\alpha|\sigma_1\rangle + \overline{\alpha}|\sigma_3\rangle$ at y is

$$[\alpha\sigma_1 + \overline{\alpha}\sigma_3]_y = \frac{1}{3}\big(-\frac{\omega}{2}\big)\omega^{Q_1(y)} + \frac{1}{3}\big(-\frac{\omega^2}{2}\big)\omega^{2Q_1(y)} = -\frac{1}{6}\big(\omega^r + \omega^{2r}\big), \qquad r = 1 + Q_1(y) \pmod 3. \tag{56}$$

Since $1 + \omega + \omega^2 = 0$, $\omega^r + \omega^{2r}$ equals 2 when $r = 0$ and -1 when $r \in \{1,2\}$; noting $r = 0$ iff $Q_1(y) = 2$,

$$[\alpha\sigma_1 + \overline{\alpha}\sigma_3]_y = \frac{1}{6}c_N(Q_1(y)). \tag{57}$$

Adding the contribution $\delta_{y,(2,2)}$ from $|\sigma_2\rangle$,

$$[\alpha\sigma_1 + \sigma_2 + \overline{\alpha}\sigma_3]_y = \frac{1}{6}c_N(Q_1(y)) + \delta_{y,(2,2)}. \tag{58}$$

Comparing with $[|\mathbb{N}\rangle^{\otimes 2}]_y = (1/6)c_N(y_0)c_N(y_1)$ from (50), (53) reduces to the single identity

$$c_N(y_0)c_N(y_1) - c_N(Q_1(y)) = 6[y = (2,2)]. \tag{59}$$

Using $c_N(y) = 1 - 3[y = 2]$ and (55),

$$c_N(y_0)c_N(y_1) = 1 - 3[y_0 = 2] - 3[y_1 = 2] + 9[y_0 = y_1 = 2], \tag{60}$$

$$c_N(Q_1(y)) = 1 - 3[Q_1(y) = 2] = 1 - 3[y_0 = 2] - 3[y_1 = 2] + 3[y_0 = y_1 = 2], \tag{61}$$

so their difference is $6[y_0 = y_1 = 2] = 6[y = (2,2)]$, establishing (59) and hence (53). Therefore $\chi(|\mathbb{N}\rangle^{\otimes 2}) \le 3$.

Machine-checked Lean formalization: `NorrellM2Pointwise.lean`. □

C.3.2 $\chi(|\mathbb{N}\rangle^{\otimes 3}) \le 4$

Proof that $\chi(|\mathbb{N}\rangle^{\otimes 3}) \le 4$. Define four 3-qutrit stabilizer states by (1):

$$\begin{aligned}
&|\sigma_1\rangle : k = 2, x_0 = (2,0,0), W = (e_1, e_2), Q_1(w) = w_0 + 2w_0^2 + 2w_1 + w_1^2 \pmod 3,\\
&|\sigma_2\rangle : k = 2, x_0 = (0,2,0), W = (e_0, e_2), Q_2(w) = 2w_0 + w_0^2 + w_1 + 2w_1^2 \pmod 3,\\
&|\sigma_3\rangle : k = 3, x_0 = 0, W = I_3, Q_3 = 0, \quad \text{so } |\sigma_3\rangle = |+\rangle^{\otimes 3},\\
&|\sigma_4\rangle : k = 2, x_0 = (0,0,2), W = (e_0, e_1), Q_4(w) = w_0 + 2w_0^2 + 2w_1 + w_1^2 \pmod 3.
\end{aligned} \tag{62}$$

We claim

$$|\mathbb{N}\rangle^{\otimes 3} = -\frac{\sqrt{6}}{4}\big(|\sigma_1\rangle + |\sigma_2\rangle + |\sigma_4\rangle\big) + \frac{\sqrt{2}}{4}|\sigma_3\rangle. \tag{63}$$

By the reduction identities (51), on the supports

$$\mathrm{supp}(\sigma_1) = \{(2, y_1, y_2)\}, \quad \mathrm{supp}(\sigma_2) = \{(y_0, 2, y_2)\}, \quad \mathrm{supp}(\sigma_4) = \{(y_0, y_1, 2)\}, \tag{64}$$

the phase polynomials reduce to

$$Q_1(y) = [y_1{=}2] + 2[y_2{=}2], \quad Q_2(y) = 2[y_0{=}2] + [y_2{=}2], \quad Q_4(y) = [y_0{=}2] + 2[y_1{=}2] \pmod 3. \tag{65}$$

Setting $a_i = [y_i = 2] \in \{0,1\}$ for $i \in \{0,1,2\}$ (consistent with the Norrell m=4 proof below), the right side of (63) at any y depends only on $a = (a_0, a_1, a_2)$ and equals

$$\text{RHS at } y = \frac{\sqrt{6}}{36} - \frac{\sqrt{6}}{12}B, \qquad B = a_0\omega^{a_1+2a_2} + a_1\omega^{2a_0+a_2} + a_2\omega^{a_0+2a_1}, \tag{66}$$

the leading $\sqrt{6}/36$ coming from $\alpha_3[\sigma_3]_y = \frac{\sqrt{2}}{4\sqrt{27}}$, and B collecting the contributions from $\sigma_1, \sigma_2, \sigma_4$ each scaled by $\alpha_j/3 = -\sqrt{6}/12$.

The sum B depends only on $n_2 = a_0 + a_1 + a_2 = |\{i : y_i = 2\}|$: it vanishes when $a = (0,0,0)$; for each of the three $n_2 = 1$ subsets exactly one term contributes $\omega^0 = 1$; for each of the three $n_2 = 2$ subsets two terms contribute $\omega^A + \omega^B$ with $\{A, B\} = \{1, 2\}$, summing to $\omega + \omega^2 = -1$; and for $a = (1,1,1)$ all three terms equal $\omega^3 = 1$, summing to 3. Therefore

$$B(n_2) = (0, 1, -1, 3) \quad \text{for } n_2 = 0, 1, 2, 3, \tag{67}$$

and substituting into (66),

$$\text{RHS}_{n_2} = \frac{\sqrt{6}}{36}\big(1 - 3B(n_2)\big) = \frac{\sqrt{6}}{36}(-2)^{n_2}, \tag{68}$$

which matches $[|\mathbb{N}\rangle^{\otimes 3}]_y$ from (50) term-for-term. This establishes (63).

Machine-checked Lean formalization: `NorrellM3.lean`, `NorrellM3Pointwise.lean`. □

C.3.3 $\chi(|\mathbb{N}\rangle^{\otimes 4}) \le 7$

Proof that $\chi(|\mathbb{N}\rangle^{\otimes 4}) \le 7$. Let $\xi = e^{i\pi/6}$, a primitive 12th root of unity, so that $\xi^4 = \omega$, $\xi^8 = \omega^2$, $\xi^3 = i$, $\xi^6 = -1$, and $\xi^{12} = 1$. Define seven 4-qutrit stabilizer states by (1); the canonical-form data $(k_j, x_{0,j}, W_j, Q_j)$ for $j = 0, 1, \ldots, 6$ are

$$\begin{aligned}
&|\sigma_0\rangle : k = 3, x_0 = (0,2,0,0), W = (e_0, e_2, e_3), Q_0(w) = 2w_0 + w_0^2 + w_1 + 2w_1^2 + 2w_2 + w_2^2,\\
&|\sigma_1\rangle : k = 4, x_0 = 0, W = I_4, Q_1(y) = \sum_{i=0}^{1}(2y_i + y_i^2) + \sum_{i=2}^{3}(y_i + 2y_i^2),\\
&|\sigma_2\rangle : k = 2, x_0 = (2,0,0,2), W = (e_1, e_2), Q_2(w) = w_0 + 2w_0^2 + w_1 + 2w_1^2,\\
&|\sigma_3\rangle : k = 2, x_0 = (0,0,2,2), W = (e_0, e_1), Q_3(w) = 2w_0 + w_0^2 + w_1 + 2w_1^2,\\
&|\sigma_4\rangle : k = 3, x_0 = (2,0,0,0), W = (e_1, e_2, e_3), Q_4(w) = 2w_0 + w_0^2 + 2w_1 + w_1^2 + w_2 + 2w_2^2,\\
&|\sigma_5\rangle : k = 2, x_0 = (0,2,2,0), W = (e_0, e_3), Q_5(w) = w_0 + 2w_0^2 + 2w_1 + w_1^2,\\
&|\sigma_6\rangle : k = 4, x_0 = 0, W = I_4, Q_6 = 0, \quad \text{so } |\sigma_6\rangle = |+\rangle^{\otimes 4}.
\end{aligned} \tag{69}$$

Setting $\tau = \sqrt{3}/4$, we claim

$$|\mathbb{N}\rangle^{\otimes 4} = \tau\omega|\sigma_0\rangle + \tau\xi|\sigma_1\rangle + \tau\xi|\sigma_2\rangle + \tau\xi|\sigma_3\rangle + \tau\omega|\sigma_4\rangle + \tau\xi|\sigma_5\rangle + \frac{1}{4}\omega^2|\sigma_6\rangle. \tag{70}$$

The seven coefficients take only three distinct values ($\tau\omega$, $\tau\xi$, $\omega^2/4$), each a 12th-root-of-unity multiple of a real number.

By the reduction identities (51), on each basis state's support the polynomial Q_j collapses to an indicator-only expression. Setting $a_i = [y_i = 2] \in \{0,1\}$,

$$\begin{aligned}
\operatorname{supp}(\sigma_0) = \{y_1 = 2\}: &\quad Q_0(y) \equiv 2a_0 + a_2 + 2a_3 \pmod 3,\\
\operatorname{supp}(\sigma_1) = \mathbb{F}_3^4: &\quad Q_1(y) \equiv 2a_0 + 2a_1 + a_2 + a_3 \pmod 3,\\
\operatorname{supp}(\sigma_2) = \{y_0 = y_3 = 2\}: &\quad Q_2(y) \equiv a_1 + a_2 \pmod 3,\\
\operatorname{supp}(\sigma_3) = \{y_2 = y_3 = 2\}: &\quad Q_3(y) \equiv 2a_0 + a_1 \pmod 3,\\
\operatorname{supp}(\sigma_4) = \{y_0 = 2\}: &\quad Q_4(y) \equiv 2a_1 + 2a_2 + a_3 \pmod 3,\\
\operatorname{supp}(\sigma_5) = \{y_1 = y_2 = 2\}: &\quad Q_5(y) \equiv a_0 + 2a_3 \pmod 3.
\end{aligned} \tag{71}$$

Every component of the right side of (70) therefore depends on y only through $a = (a_0, a_1, a_2, a_3) \in \{0,1\}^4$. Writing $\mathbf{1}_j(a) \in \{0,1\}$ for the indicator that a lies in $\operatorname{supp}(\sigma_j)$, the right-hand side amplitude is

$$\mathrm{RHS}(a) = \sum_{j=0}^{6} \alpha_j 3^{-k_j/2} \omega^{Q_j(a)} \mathbf{1}_j(a), \tag{72}$$

with the α_j as in (70) and k_j as in (69).

Endpoints. At $a = (0,0,0,0)$ only $|\sigma_1\rangle$ and $|\sigma_6\rangle$ have a in their support, so

$$\mathrm{RHS}(0,0,0,0) = \frac{\tau\xi}{9}\omega^0 + \frac{\omega^2}{36}\omega^0 = \frac{1}{36}\big(\sqrt{3}\xi + \omega^2\big). \tag{73}$$

Since $\sqrt{3}\xi = \frac{3}{2} + i\frac{\sqrt{3}}{2}$ and $\omega^2 = -\frac{1}{2} - i\frac{\sqrt{3}}{2}$, the sum equals 1, so $\mathrm{RHS}(0,0,0,0) = 1/36$.

At $a = (1,1,1,1)$ all seven basis states contribute. After evaluating Q_j in each case (using $\xi^4 = \omega$ and $\tau\omega\omega^2 = \tau$), the seven contributions collect to

$$\begin{aligned}
\mathrm{RHS}(1,1,1,1) &= \frac{1}{12} + \frac{\sqrt{3}\xi}{36} + \frac{(-i)\tau}{3} + \frac{\sqrt{3}\xi}{12} + \frac{1}{12} + \frac{\sqrt{3}\xi}{12} + \frac{\omega^2}{36}\\
&= \frac{1}{36}\big(6 + 7\sqrt{3}\xi - 3i\sqrt{3} + \omega^2\big).
\end{aligned} \tag{74}$$

Substituting $7\sqrt{3}\xi = \frac{21}{2} + i\frac{7\sqrt{3}}{2}$ and collecting reals/imaginaries yields $6 + \frac{21}{2} - \frac{1}{2} - 0 = 16$ and $\frac{7\sqrt{3}}{2} - 3\sqrt{3} - \frac{\sqrt{3}}{2} = 0$, so $\mathrm{RHS}(1,1,1,1) = 16/36 = 4/9$.

Intermediate cases. Direct enumeration over the remaining 14 patterns $a \in \{0,1\}^4$ with $n_2(a) = \sum_i a_i \in \{1,2,3\}$ analogously reduces $\mathrm{RHS}(a)$ to a polynomial identity in ξ over $\mathbb{Z}[\sqrt{3}]$, decided by $\xi^4 = \omega$, $\xi^6 = -1$, and $1 + \omega + \omega^2 = 0$. Across the 14 patterns, $\mathrm{RHS}(a)$ depends only on $n_2(a) \in \{1,2,3\}$: the coefficient pattern in Eq. (70) and the reduced phases in (71) are jointly invariant under the symmetric-group action that permutes the four coordinates of a within each n_2-class, so the 4, 6, and 4 patterns in classes $n_2 = 1,2,3$ each yield the same value. The two representatives below cover $n_2 = 1$ and $n_2 = 2$; the same mechanism handles $n_2 = 3$ and the remaining patterns in each class.

Case $n_2 = 1$, $a = (1,0,0,0)$. Only $|\sigma_1\rangle, |\sigma_4\rangle, |\sigma_6\rangle$ have a in their support; reading off the reduced phases (71), $Q_1(a) = 2$, $Q_4(a) = 0$, $Q_6 = 0$, so the contributions are $\tau\xi\omega^2/9 = -i\sqrt{3}/36$, $\tau\omega 1/(3\sqrt{3}) = \omega/12$, and $\omega^2/41/9 = \omega^2/36$, respectively. Summing,

$$\mathrm{RHS}(1,0,0,0) = \frac{1}{36}\big(-i\sqrt{3} + 3\omega + \omega^2\big) = -\frac{1}{18}, \tag{75}$$

using $-i\sqrt{3}+3\omega+\omega^2 = -i\sqrt{3}+3(-\frac{1}{2}+i\frac{\sqrt{3}}{2})+(-\frac{1}{2}-i\frac{\sqrt{3}}{2}) = -2$.

Case $n_2 = 2$, $a = (1,1,0,0)$. The supports containing this pattern are $|\sigma_0\rangle, |\sigma_1\rangle, |\sigma_4\rangle, |\sigma_6\rangle$; $Q_0(a) = 2$, $Q_1(a) = 4 \equiv 1$, $Q_4(a) = 2$, $Q_6 = 0$, so the four contributions are $\tau\omega\omega^2/(3\sqrt{3}) = 1/12$, $\tau\xi\omega/9 = \xi\omega\sqrt{3}/36$, $\tau\omega\omega^2/(3\sqrt{3}) = 1/12$, and $\omega^2/41/9 = \omega^2/36$. Summing,

$$\mathrm{RHS}(1,1,0,0) = \frac{1}{36}\big(6+\xi\omega\sqrt{3}+\omega^2\big) = \frac{1}{9}, \tag{76}$$

using $\xi\omega = e^{i5\pi/6}$, hence $\xi\omega\sqrt{3} = -\frac{3}{2}+i\frac{\sqrt{3}}{2}$, which combines with ω^2 to give -2.

All 16 cases. The remaining 12 patterns are verified by the same mechanism. The $\mathrm{RHS}(a)$ value depends only on $n_2(a)$, and matches the target $(-2)^{n_2(a)}/36$ in each n_2-class:

$n_2(a)$	# patterns	$\mathrm{RHS}(a)$	target $(-2)^{n_2}/36$
0	1	$1/36$	$1/36$
1	4	$-1/18$	$-1/18$
2	6	$1/9$	$1/9$
3	4	$-2/9$	$-2/9$
4	1	$4/9$	$4/9$

All 16 scalar identities are checked at exact rational precision and the pointwise identity is independently formalized in Lean 4 (Section 4). Comparing with the target amplitude $[|\mathbb{N}\rangle^{\otimes 4}]_y = (-2)^{n_2(y)}/36$ from (50) establishes (70), and hence $\chi(|\mathbb{N}\rangle^{\otimes 4}) \le 7$.

Machine-checked Lean formalization: `NorrellM4Pointwise.lean`. □

C.4 Qubit T-type $m = 4$ decomposition

The qubit T-type orbit of [BK05] is represented by

$$|T\rangle = \cos\beta|0\rangle + e^{i\pi/4}\sin\beta|1\rangle, \qquad \cos(2\beta) = \frac{1}{\sqrt{3}}, \tag{77}$$

from which $\cos^2\beta = (1+1/\sqrt{3})/2$, $\sin^2\beta = (1-1/\sqrt{3})/2$, and $\cos\beta\sin\beta = 1/\sqrt{6}$.

Proposition 8. *For $x \in \mathbb{F}_2^4$ define the three 4-qubit stabilizer states*

$$\begin{aligned}
|\sigma_1\rangle &= 2^{-3/2}\sum_{x_1=x_3} i^{x_1}(-1)^{x_2x_4}|x\rangle,\\
|\sigma_2\rangle &= 2^{-2}\sum_{x\in\mathbb{F}_2^4} i^{x_2+x_4}(-1)^{x_1x_3+x_2x_4}|x\rangle,\\
|\sigma_3\rangle &= 2^{-3/2}\sum_{x_2=x_4} i^{x_1+x_2+x_3}(-1)^{x_1x_3}|x\rangle,
\end{aligned} \tag{78}$$

with linear coefficients

$$c_1 = \frac{2}{3}e^{i\pi/12}, \qquad c_2 = \frac{2}{3}, \qquad c_3 = \frac{2}{3}e^{-i\pi/12}. \tag{79}$$

Then

$$|T\rangle^{\otimes 4} = c_1|\sigma_1\rangle + c_2|\sigma_2\rangle + c_3|\sigma_3\rangle, \tag{80}$$

hence $\chi(|T\rangle^{\otimes 4}) = 3$ (tight via monotonicity from the $m = 3$ lower-bound certificate) and $\gamma_T \le \log_2(3)/4 \approx 0.396$.

Proof. The amplitude of $|T\rangle^{\otimes 4}$ at $|x\rangle$ depends only on the Hamming weight $w = x_1 + x_2 + x_3 + x_4$ and equals $\cos^{4-w}\beta \sin^w \beta e^{i\pi w/4}$. Reducing via $\cos^2\beta = (1 + 1/\sqrt{3})/2$, $\sin^2\beta = (1 - 1/\sqrt{3})/2$, $\cos\beta\sin\beta = 1/\sqrt{6}$,

$$\left[|T\rangle^{\otimes 4}\right]_x = \begin{cases} (2+\sqrt{3})/6 & w = 0, \\ (\sqrt{3}+1)(1+i)/12 & w = 1, \\ i/6 & w = 2, \\ (\sqrt{3}-1)(-1+i)/12 & w = 3, \\ (\sqrt{3}-2)/6 & w = 4. \end{cases} \tag{81}$$

Set $a = [x_1 = x_3]$ and $b = [x_2 = x_4]$. From the support conditions in (78), σ_1 vanishes off $\{a = 1\}$ and σ_3 off $\{b = 1\}$, while σ_2 has full support. The right-hand side of (80) therefore splits into four support classes by $(a, b) \in \{0, 1\}^2$. Throughout we use

$$\cos\frac{\pi}{12} = \frac{\sqrt{6}+\sqrt{2}}{4}, \quad \sin\frac{\pi}{12} = \frac{\sqrt{6}-\sqrt{2}}{4}, \quad \cos\frac{\pi}{12} - \sin\frac{\pi}{12} = \frac{1}{\sqrt{2}}, \tag{82}$$

which together give the useful identity

$$\frac{e^{i\pi/12}}{3\sqrt{2}} = \frac{\sqrt{3}+1}{12} + i\frac{\sqrt{3}-1}{12}. \tag{83}$$

Case $(a, b) = (0, 0)$**.** Every x in this class has $w = 2$, $x_1x_3 = 0$, $x_2x_4 = 0$, and $x_2 + x_4 = 1$, so the only contributing term is

$$[c_2\sigma_2]_x = \frac{2}{3}\frac{1}{4} i(-1)^0 = \frac{i}{6}, \tag{84}$$

matching the $w = 2$ target.

Case $(a, b) = (1, 1)$**.** Write $x_1 = x_3 = p$ and $x_2 = x_4 = q$ with $p, q \in \{0, 1\}$; $w = 2(p + q)$. The four sub-classes are listed below; in each row the right-most column collapses via (82).

(p, q)	$[\sigma_1]_x$	$[\sigma_2]_x$	$[\sigma_3]_x$	$\sum_j c_j[\sigma_j]_x$
$(0,0)$	$\frac{1}{2\sqrt{2}}$	$\frac{1}{4}$	$\frac{1}{2\sqrt{2}}$	$\frac{2\cos(\pi/12)}{3\sqrt{2}} + \frac{1}{6} = \frac{2+\sqrt{3}}{6}$
$(0,1)$	$-\frac{1}{2\sqrt{2}}$	$\frac{1}{4}$	$\frac{i}{2\sqrt{2}}$	$\frac{(\cos-\sin)(\pi/12)}{3\sqrt{2}}(i-1) + \frac{1}{6} = \frac{i}{6}$
$(1,0)$	$\frac{i}{2\sqrt{2}}$	$-\frac{1}{4}$	$\frac{1}{2\sqrt{2}}$	$\frac{(\cos-\sin)(\pi/12)}{3\sqrt{2}}(1+i) - \frac{1}{6} = \frac{i}{6}$
$(1,1)$	$-\frac{i}{2\sqrt{2}}$	$-\frac{1}{4}$	$\frac{i}{2\sqrt{2}}$	$\frac{2\sin(\pi/12)}{3\sqrt{2}} - \frac{1}{6} = \frac{\sqrt{3}-2}{6}$

Each row matches the $w \in \{0, 2, 2, 4\}$ target.

Case $(a, b) = (1, 0)$**.** Only σ_1 and σ_2 contribute. Writing $x_1 = x_3 = p$ and $x_2 \neq x_4$ gives $[\sigma_1]_x = i^p/(2\sqrt{2})$ and $[\sigma_2]_x = i(-1)^p/4$, so

$$p = 0 (w = 1): \quad [c_1\sigma_1 + c_2\sigma_2]_x = \frac{e^{i\pi/12}}{3\sqrt{2}} + \frac{i}{6} = \frac{(\sqrt{3}+1)(1+i)}{12}, \tag{85}$$

$$p = 1 (w = 3): \quad [c_1\sigma_1 + c_2\sigma_2]_x = \frac{ie^{i\pi/12}}{3\sqrt{2}} - \frac{i}{6} = \frac{(\sqrt{3}-1)(-1+i)}{12}, \tag{86}$$

using (83) in each line; these match the $w = 1$ and $w = 3$ targets.

Case $(a,b) = (0,1)$**.** Only σ_2 and σ_3 contribute. Writing $x_2 = x_4 = q$ and $x_1 \neq x_3$ gives $i^{x_2+x_4} = i^{2q} = (-1)^q$, $(-1)^{x_1x_3+x_2x_4} = (-1)^{0+q} = (-1)^q$ (since $x_1 \neq x_3 \in \{0,1\}$ forces $x_1x_3 = 0$), so $[\sigma_2]_x = (-1)^q(-1)^q/4 = 1/4$ and $[\sigma_3]_x = i^{1+q}/(2\sqrt{2})$, so

$$q = 0 (w = 1): \quad [c_2\sigma_2 + c_3\sigma_3]_x = \frac{1}{6} + \frac{ie^{-i\pi/12}}{3\sqrt{2}} = \frac{(\sqrt{3}+1)(1+i)}{12}, \tag{87}$$

$$q = 1 (w = 3): \quad [c_2\sigma_2 + c_3\sigma_3]_x = \frac{1}{6} - \frac{e^{-i\pi/12}}{3\sqrt{2}} = \frac{(\sqrt{3}-1)(-1+i)}{12}, \tag{88}$$

using the conjugate $e^{-i\pi/12}/(3\sqrt{2}) = (\sqrt{3}+1)/12 - i(\sqrt{3}-1)/12$ of (83); again matching the $w = 1$ and $w = 3$ targets.

The four cases cover $\mathbb{F}_2^4$, so (80) holds pointwise. The exponent bound is then (6). □

Machine-checked Lean formalization: `QubitTM4.lean`.